



This is a repository copy of *Regulation, sensory domains and roles of two Desulfovibrio desulfuricans ATCC27774 Crp family transcription factors, HcpR1 and HcpR2, in response to nitrosative stress.*

White Rose Research Online URL for this paper:
<http://eprints.whiterose.ac.uk/106231/>

Version: Accepted Version

Article:

Cadby, I.T., Ibrahim, S.A., Faulkner, M. et al. (7 more authors) (2016) Regulation, sensory domains and roles of two *Desulfovibrio desulfuricans* ATCC27774 Crp family transcription factors, HcpR1 and HcpR2, in response to nitrosative stress. *Molecular Microbiology*, 102 (6). pp. 1120-1137. ISSN 0950-382X

<https://doi.org/10.1111/mmi.13540>

This is the peer reviewed version of the following article: Cadby, I. T. et al (2016), Regulation, sensory domains and roles of two *Desulfovibrio desulfuricans* ATCC27774 Crp family transcription factors, HcpR1 and HcpR2, in response to nitrosative stress. *Molecular Microbiology*, which has been published in final form at <http://dx.doi.org/10.1111/mmi.13540>. This article may be used for non-commercial purposes in accordance with Wiley Terms and Conditions for Self-Archiving

Reuse

Unless indicated otherwise, fulltext items are protected by copyright with all rights reserved. The copyright exception in section 29 of the Copyright, Designs and Patents Act 1988 allows the making of a single copy solely for the purpose of non-commercial research or private study within the limits of fair dealing. The publisher or other rights-holder may allow further reproduction and re-use of this version - refer to the White Rose Research Online record for this item. Where records identify the publisher as the copyright holder, users can verify any specific terms of use on the publisher's website.

Takedown

If you consider content in White Rose Research Online to be in breach of UK law, please notify us by emailing eprints@whiterose.ac.uk including the URL of the record and the reason for the withdrawal request.



eprints@whiterose.ac.uk
<https://eprints.whiterose.ac.uk/>

Regulation, sensory domains and roles of two *Desulfovibrio desulfuricans* ATCC27774 Crp family transcription factors, HcpR1 and HcpR2, in response to nitrosative stress

Ian T. Cadby¹, Susan A. Ibrahim², Matthew Faulkner¹, David J. Lee¹, Douglas Browning¹, Stephen J. Busby¹, Andrew L. Lovering¹, Melanie R. Stapleton², Jeffrey Green² and Jeffrey A. Cole^{1*}

School of Biosciences, University of Birmingham, Birmingham B15 2TT, UK¹ and Molecular Biology and Biotechnology, University of Sheffield, Firth Court, Western Bank, Sheffield S10 2TN, UK².

*Corresponding author:

E-mail: j.a.cole@bham.ac.uk

Tel: 44 121 414 5440

Fax: 44 121 414 5925

Key words: Crp/Fnr family proteins; *Desulfovibrio* HcpR1 and HcpR2; hybrid cluster protein; nitrosative stress; sulphate reducing bacteria

Running title: Regulation of *D. desulfuricans* NO stress by HcpR1 and HcpR2

This article has been accepted for publication and undergone full peer review but has not been through the copyediting, typesetting, pagination and proofreading process which may lead to differences between this version and the Version of Record. Please cite this article as an 'Accepted Article', doi: 10.1111/mmi.13540

Summary

In silico analyses identified a Crp/Fnr family transcription factor (HcpR) in sulfate-reducing bacteria that controls expression of the *hcp* gene, which encodes the hybrid cluster protein and contributes to nitrosative stress responses. There is only one *hcpR* gene in the model sulfate-reducing bacterium *Desulfovibrio vulgaris* Hildenborough, but two copies in *D. desulfuricans* 27774, which can use nitrate as an alternative electron acceptor to sulfate. Structures of the *D. desulfuricans hcpR1*, *hcpR2* and *hcp* operons are reported. We present evidence that *hcp* expression is regulated by HcpR2, not by HcpR1, and that these two regulators differ in both their DNA-binding site specificity and their sensory domains. HcpR1 is predicted to be a *b*-type cytochrome. HcpR1 binds upstream of the *hcpR1* operon and its synthesis is regulated coordinately with *hcp* in response to NO. In contrast, *hcpR2* expression was not induced by nitrate, nitrite or NO. HcpR2 is an iron-sulfur protein that reacts with NO and O₂. We propose that HcpR1 and HcpR2 use different sensory mechanisms to regulate subsets of genes required for defense against NO-induced nitrosative stress, and that diversification of signal perception and DNA recognition by these two proteins is a product of *D. desulfuricans* adaptation to its particular environmental niche.

Introduction

Sulfate reducing bacteria are obligate anaerobes that conserve energy during the reduction of sulfate via sulfite to sulfide. Much of the biochemical information about these bacteria has come from studies of three species of *Desulfovibrio*: *D. vulgaris*, especially strain Hildenborough; *Desulfovibrio alaskensis* strain G20 (formerly *D. desulfuricans* G20); and *D. desulfuricans*, especially strain ATCC27774. Although there are well-developed genetic systems for studying *D. vulgaris*, many attempts by us and others have failed to generate similar systems for *D. desulfuricans*. Consequently far more is known about gene function and genetic regulation in *D. vulgaris* than in *D. desulfuricans*.

Desulfovibrio vulgaris is not abundant in the human gastrointestinal tract, but is readily isolated from anaerobic soils and sediments, indicating that it has largely adapted to live outside the bodies of warm blooded animals (Rabus *et al.*, 2015). In contrast, *D. desulfuricans* and related strains are readily isolated from human faeces (Jia *et al.*, 2012). There have been suggestions that *D. desulfuricans* might be a cause of gastric disease, but there is only limited evidence for a correlation between the presence of *Desulfovibrio* species and gastric disease (Fox *et al.*, 1999; Loubinoux *et al.*, 2000; 2002; Jia *et al.*, 2012; Jia *et al.*, 2013). In contrast to *D. vulgaris*, *D. desulfuricans* and some other sulfate-reducing bacteria isolated from the human body can use anaerobic reduction of nitrate via nitrite to ammonia to conserve energy for growth (Senez and Pichinoty, 1958; Widdel and Pfennig, 1982; Keith and Herbert, 1983; McCready *et al.*, 1983; Mitchell *et al.*, 1985; Moura *et al.*, 1997; Jia *et al.*, 2012; Marietou *et al.*, 2009). *Desulfovibrio desulfuricans* is therefore exposed to nitrosative stress induced by nitric oxide (NO) from two sources: NO generated as part of host defense mechanisms; and NO generated from nitrite as a side product of nitrate and nitrite reduction. The major enzyme that generates NO from nitrite in enteric bacteria is the membrane-associated nitrate reductase, NarG, with smaller contributions from the NADH-dependent nitrite reductase, NirB, and the periplasmic nitrite reductase, NrfA (reviewed by Vine and Cole, 2011). Although NrfA is also present in *D. desulfuricans*, it synthesizes only the periplasmic nitrate reductase, NapA, which in *Salmonella enterica* has been shown not to be a major source of NO (Rowley *et al.*, 2012).

Bacteria are equipped with a range of NO detoxification mechanisms. *Escherichia coli* encodes a flavohemoglobin, Hmp, which functions as an NO dioxygenase under aerobic conditions, and a flavorubredoxin, NorV, an NO reductase under anaerobic conditions (Gardner and Gardner, 2002; Gomes *et al.*, 2002). The periplasmic nitrite reductase NrfA also functions as an NO reductase (Poock *et al.*, 2002; van Wonderen *et al.*, 2008). Thus, *E. coli* is equipped to detoxify NO under different conditions and within different cellular locations. The *hcp* gene product (hybrid-cluster protein, Hcp) has also been implicated in coping with nitrosative stress as its synthesis is induced by

NO although until recently the precise function of this enigmatic protein remained elusive (van den Berg *et al.*, 2000; Constantinidou *et al.*, 2006; Filenko *et al.*, 2007; Johnson *et al.*, 2009; Chismon *et al.*, 2010; Vine *et al.*, 2011; Seth *et al.*, 2012). We recently reported that the *Escherichia coli* Hcp is a high affinity NO reductase that is the major enzyme for reducing NO stoichiometrically to N₂O under physiologically relevant conditions. It is an extremely unstable protein that is sensitive to inactivation by oxygen and NO, but is protected by an Hcp reductase, Hcr, encoded by the second gene of the *hcp-hcr* operon (Wang *et al.*, 2016). Hcp and transcription factors required for its synthesis are required for nitric oxide resistance in *Porphyromonas gingivalis* and *Desulfovibrio vulgaris* (Boutrin *et al.*, 2012; Figueredo *et al.*, 2013; Lewis *et al.*, 2012). In *D. vulgaris* there are two copies of the *hcp* gene and mutagenesis studies indicate that each is responsible for maintaining the integrity of electron transport chains under nitrosative stress (Yurkiw *et al.*, 2012).

In sulfate-reducing bacteria, *hcp* is predicted to be regulated by the Crp (cyclic AMP receptor protein) family transcription factor, HcpR (Rodionov *et al.*, 2004; Rodionov *et al.*, 2005). Induction of *hcp* in response to nitrite or NO in *D. vulgaris*, *D. gigas* and *Porphyromonas gingivalis* is HcpR-dependent (Lewis *et al.*, 2012; Zhou *et al.* 2012; da Silva *et al.*, 2015). The *in vitro* binding of *P. gingivalis* HcpR to *hcp* promoter DNA was demonstrated to be heme-dependent, but the HcpR of this species has limited sequence similarity to those of proteobacteria such as *Desulfovibrio* species (Lewis *et al.*, 2012). Although multiple reports have predicted target DNA sequences for HcpR proteins, none of them has been verified experimentally and how the HcpR proteins of proteobacteria sense nitrosative stress is unknown.

In *D. desulfuricans* 27774, two paralogues of HcpR, Ddes_0528 and Ddes_1827, are present (Cadby *et al.*, 2011). These proteins are referred to as HcpR1 and HcpR2, respectively. We show that the two paralogues of HcpR differ not only in DNA-binding site specificity, but also in their sensor domains. We propose that HcpR1 is a heme-binding *b*-type cytochrome that is tightly

regulated in response to nitrosative stress. Its paralogue, HcpR2, is an iron-sulfur protein; its synthesis is not induced during growth in the presence of nitrate, nitrite, sulfite or NO.

Results

Diversity in the HcpR family

HcpR1 is representative of the HcpR proteins found in other *Desulfovibrio* species with a predicted DNA target site identical to the consensus DNA target site of *E. coli* Crp. This prediction is based upon the presence of R, E and R residues at positions 1, 2 and 6 of the DNA recognition helix (Fig. S1). In contrast, the HcpR2 of *D. desulfuricans* is not found in other *Desulfovibrio* species and its DNA recognition helix with a proline instead of a glutamate at position 2 is similar to the HcpR proteins found in *Clostridium* and *Bacteroides* species (Rodionov *et al.*, 2005). Although numerous other sulfate-reducing bacteria also encode two HcpR paralogues, it is intriguing that the HcpR2 of *D. desulfuricans* shows great sequence divergence throughout the protein from the HcpR proteins of close relatives in terms of their 16S rRNA sequence similarity (da Silva *et al.* 2015; Fig. S1).

In addition to this sequence divergence, the genomic localization of the *D. desulfuricans* *hcpR* genes also differ from those of other *Desulfovibrio* species. In many sulfate-reducing bacteria including *D. vulgaris* Hildenborough and *D. alaskensis* strain G20, the *hcp* gene is located close to and convergent upon *hcpR* (Fig. 1a). Immediately upstream from the *hcp* gene is an inverted repeat sequence almost identical to consensus binding sites in *E. coli* for Crp. The *hcp* gene in these species is located adjacent to two other genes, *frdX* and *adhE*, suggesting that they might be in an operon with *hcp* that is regulated by HcpR (Rodionov *et al.*, 2005; da Silva *et al.*, 2015). In *D. gigas*, the *hcpR* gene is located in a distinct transcription unit divergent with the *hcp* operon. There are putative HcpR binding sites between the *hcp* and *hcpR* genes, and also upstream of the distantly located *frdX* gene (Fig. 1a). In contrast, in some nitrate-reducing *Desulfovibrio* species the *hcp* gene is in a putative operon with *hcpR* and two uncharacterized genes, *wrbA* and *nimA*, suggesting that expression of *hcpR* would be regulated co-coordinately with *hcp* in these species (Fig.1b).

Intriguingly, in *D. desulfuricans*, the *hcpR1* gene seems to be in an operon with *wrbA* and *nimA*, but the *hcp* gene is absent, instead being at a distant locus downstream from the *hcpR2* gene (Fig. 1c).

Although the *D. desulfuricans hcp* gene is not linked to *hcr*, genes for iron-sulfur proteins are abundant in this bacterium, one of which, *frdX*, is located close to the *hcp* gene. It is therefore possible that FrdX or another iron-sulfur protein protects *D. desulfuricans* Hcp from inactivation by NO. The arrangement of genes at the *D. desulfuricans hcp* locus is syntenous with those of some *Clostridium* species (Fig. 1d). Although no inverted repeat sequences were found immediately upstream from *hcpR2* in *D. desulfuricans*, a potential binding site for HcpR2 was found between the *hcpR2* and *hcp* genes, suggesting that *hcpR2* and *hcp* might be expressed independently of one another.

Confirmation of the hcpR1 and hcpR2 operon structures

In *D. desulfuricans* 27774, the *hcpR1* gene is the first gene of a potential three-gene operon that includes genes annotated as encoding a flavodoxin and a pyridoxamine oxidase (Fig. 1c). The sequences of these proteins were analyzed by threading (Kelley *et al.*, 2015) using the PHYRE2 server and are likely to adopt protein folds similar to the tryptophan repressor protein, WrbA, and the nitroimidazole reductase, NimA. Similarly, *hcpR2* could also be in an operon with downstream genes Ddes_1828, annotated as encoding a cupin domain protein, and *hcp* (Fig. 1c). In agreement with the gene annotation, threading also suggested that this middle gene adopts a cupin fold similar to YlbA of *E. coli*.

To investigate whether the *hcpR* genes of *D. desulfuricans* are co-transcribed with their genomic neighbors, the structures of the *hcpR* operons were determined by RT-PCR. The expression of these genes in response to nitrosative stress was then investigated. Reverse transcriptase-PCR with random hexamers was used to generate cDNA from RNA isolated from nitrate-grown *D. desulfuricans*. This cDNA was used in a conventional PCR strategy using sixteen primer pairs to determine whether the *hcpR1* gene is co-transcribed with the *wrbA* and *nimA* genes and whether

hcpR2 is co-transcribed with *ylbA* and *hcp* (Fig. 2a). All primer combinations amplified the predicted regions of genomic DNA (Fig. 2b top panel). At the *hcpR1* locus, transcripts of each individual gene were readily detected, as were transcripts spanning the gene boundaries. As a negative control, no transcript extending 300 bp upstream from the *hcpR1* gene was detected. Similarly, all of the predicted mRNA fragments corresponding to co-transcription of the *hcpR2*, *ylbA* and *hcp* genes were detected, with no cDNA resulting from transcripts extending upstream from the *hcpR2* gene. No DNA product was detected in controls from which reverse transcriptase was omitted. Although qRT-PCR was not used for this experiment, the *ylbA-hcp* transcript seemed to be particularly abundant as judged by the intensity of the PCR products on the agarose gel (Fig. 2b, Lane L, bottom panel). The combined data indicate that the *hcpR1* and *hcpR2* genes can be co-transcribed as operons with their genomic neighbors and that *hcp* transcription in *D. desulfuricans* might be regulated by the product of the first gene of the *hcp* operon, HcpR2, but not by HcpR1.

Regulation of expression of the hcpR1 and hcpR2 genes

To determine whether expression of *hcpR1* or *hcpR2* is regulated by the terminal electron acceptor available during growth, *D. desulfuricans* cultures from a sulfate-grown inoculum were transferred to fresh medium in which 7.5 mM sulfate or nitrate was supplied as the only terminal electron acceptor. A third set of cultures was supplemented with 2.5 mM nitrite, which partially inhibited growth. Similar growth yields were obtained from the sulfate and nitrate cultures after 22 h, but after 44 h higher yields were obtained from the nitrate-grown cultures, as reported previously by Marietou et al. (2009). RNA was extracted from each of the cultures during the exponential phase of growth and the levels of the *hcpR1* and *hcpR2* transcripts in these cultures were compared with expression of the *hcp* gene (Fig. 3a). During growth in the presence of nitrate as the only electron acceptor, expression of *hcpR1* was induced 50-fold relative to a sulfate-grown control culture, and *hcp* expression was induced 8-fold. Even higher levels, 140-fold induction of *hcpR1* and 30-fold induction of *hcp* relative to the sulfate culture were detected in cultures grown with nitrite as the

terminal electron acceptor (Fig. 3a). In contrast to the strong induction of *hcpR1* expression during growth in the presence of nitrate or nitrite, expression of *hcpR2* was unaffected, or at most only slightly affected, by the availability of different terminal electron acceptors during growth (Fig. 3b).

The induction of *hcpR1* synthesis by nitrate and even greater induction by nitrite is similar to the derepression of NsrR-regulated genes in *E. coli* by NO generated as a side product of nitrite reduction to ammonia (Constantinidou *et al.*, 2006; Vine and Cole, 2011). To determine whether *D. desulfuricans* *hcpR1* or *hcpR2* transcription is induced by NO, sulfate-grown inocula were transferred to fresh medium in which 15 mM sulfate was supplied as the only terminal electron acceptor. Cultures were grown to an OD₆₀₀ of 0.25-0.3 and were then supplemented with 7.5 μM NO or an equivalent volume of water. The addition of NO to cultures resulted in a brief lag in growth followed by recovery. After 20 h, cells were harvested and RNA was extracted. The *hcpR1* and *hcpR2* transcripts in these cultures were compared by qRT-PCR analysis (Fig. 4a). Following NO treatment, expression of *hcpR1* was induced 7-fold relative to cultures that had been supplemented with water. In contrast to the strong induction of *hcpR1* expression during NO stress, expression of *hcpR2* was unaffected, or at most only slightly affected by NO added during growth. Similar data were obtained from cultures harvested after only 4 h exposure to NO, so the failure of *hcpR2* expression to respond to nitrate, nitrite or NO after 20 h was not due to inadequate exposure to nitrosative stress. This result, in addition to the clear response of *hcpR1* expression 20 h after the addition of NO, strongly suggests that *hcpR1* expression is induced by NO, but expression of *hcpR2* is not regulated by nitrate, nitrite or NO.

We next checked whether *hcp* expression correlates with the expression of either *hcpR1* or *hcpR2*. The data showed that *hcp* expression was induced >50-fold during growth in the presence of NO (Fig. 4b). Thus, the expression data indicated that both *hcpR1* and *hcp* respond to nitrosative stress. Expression of *hcpR2* and *hcp* are not regulated similarly, and there is a candidate HcpR2 binding site between the *hcpR2* and *ylbA* genes, but not upstream of *hcpR2*. We therefore suggest

that *hcp* is transcribed from two different promoters, one upstream of the *hcpR2* and another downstream of this gene.

Effects of nitric oxide stress on the intracellular concentration of HcpR1

The experiments described above indicated that NO induces expression of *hcpR1* but not *hcpR2*.

To establish whether this transcription regulation elicited changes at the protein level, Western blotting using antisera raised against purified HcpR1 protein was used to monitor the intracellular concentrations of protein in bacteria grown in the presence of different concentrations of NO. Cultures of *D. desulfuricans* that had been grown with sulfate as the electron acceptor were transferred into fresh media in which 7.5 mM sulfate was supplied as the sole terminal electron acceptor. Growth was monitored by measuring optical density and after 18 h, during exponential growth, the cultures were supplemented with 5 or 25 μ M NO or, as a negative control, water (Fig. 5a). *Desulfovibrio desulfuricans* cells grown on sulfate and supplemented with water grew unchecked and reached stationary phase (Fig. 5a, grey circles). The addition of 5 μ M NO (Fig. 5a, black diamonds) resulted in a brief interruption in growth but final optical densities were comparable to control cultures. Treatment with 25 μ M NO compromised the cells more seriously, resulting in a prolonged lag in growth and lower final optical densities (Fig. 5a, grey triangles).

Cell samples were taken immediately prior to the addition of NO and also 4, 24 and 50 h following supplementation. Standardized protein samples prepared from harvested cells were resolved by SDS-PAGE and the levels of HcpR1 were probed by Western blotting (Fig. 5b). Consistent with the qRT-PCR results, negligible quantities of HcpR1 were detected in bacteria from cultures grown with sulfate prior to the addition of NO. A strong band of HcpR1 protein was detected 4 hours after the addition of 5 μ M NO, with similar quantities being present after 24 and 50 h. Similar levels of HcpR1 accumulated in cultures treated with 25 μ M NO after 24 and 50 hours, but not after 4 hours. Presumably, the acute stress initially caused by this concentration of NO resulted in inhibition of protein synthesis. HcpR1 synthesis remained negligible in control

cultures throughout the experiment (Fig. 5b). Collectively the data indicate that *D. desulfuricans* is sensitive to exogenous NO, which stimulates production of the HcpR1 protein.

HcpR1 is a DNA-binding protein

Bioinformatic analyses predicted that HcpR1 would bind to several targets throughout the *D. desulfuricans* genome (Marietou *et al.*, 2009; Cadby *et al.*, 2011). These include the promoters of the *nap* operon, which encodes the periplasmic nitrate reductase, and the *sat* gene encoding ATP sulfurylase. The HcpR1 binding site at the *hcpR1* promoter is a perfect inverted repeat and represents the best match to the HcpR1 consensus sequence in the *D. desulfuricans* genome (Fig. 6a). Potential -10 and -35 promoter elements were also identified for *hcpR1* using the Softberry BPROM tool, suggesting that the HcpR1 binding site is centered between bases 61 and 62 before the putative transcription start site, similar to the positioning of *E. coli* CRP at a typical class I promoter (Ebright, 1993). The *hcpR1* coding sequence amplified by PCR using genomic DNA as the template was cloned into the pET21a expression vector (Novagen) to yield plasmid pETHcpR1 and transformed into *E. coli* strain BL21 (DE3). Purified transformants were grown aerobically, induced with a low concentration (50 μ M) IPTG and the N-terminally His-tagged recombinant HcpR1 protein was purified by Ni⁺⁺ affinity chromatography. Different concentrations of purified HcpR1 were incubated with a ³²P end-labeled DNA fragment covering the *hcpR1* promoter and regulatory region. Protein-DNA complexes were separated from unbound DNA by non-denaturing PAGE and visualized by autoradiography (Fig. 6b). A single high affinity complex was detected even at the lowest concentration of HcpR1 indicating that the protein binds to a single site in the *hcpR1* regulatory region.

Evidence that HcpR1 might be heme-protein

As isolated, the HcpR1 protein appears to lack co-factors, as judged by UV-visible spectroscopy. A multiple alignment of predicted HcpR1 proteins from 18 different sulfate-reducing bacteria was constructed to identify conserved residues. From the position of conserved residues on structural

models of HcpR1 generated with PHYRE2, it was noticed that a number of conserved or semi-conserved residues (Leu-80, Phe-61, Arg-82, Val-78, Lys-79, Leu-73, a hydrophobic residue at position 10, Pro-113) are located proximal to strictly conserved His-93 (Kelley *et al.*, 2015). These residues were recognized as potential ligands for a heme *b* prosthetic group (Schneider *et al.*, 2007). Titration of HcpR1 with hemin resulted in a UV-visible spectrum with an absorbance maximum at 415 nm and a broad band around 535 nm indicating that hemin was bound by the protein (Fig. 7a). Plots of the absorbance at 415 nm (relative to absorbance at 280 nm) against the ratio of hemin to protein revealed that HcpR1 binds hemin with a stoichiometry of approximately 1 hemin per mole of HcpR1 monomer (Fig. 7b). The absorbance spectrum of a sample of HcpR1 reconstituted with hemin was measured before and after reduction with dithionite. On reduction, the maxima at 415 and 535 nm were replaced by sharper bands at 425, 530 and 560 nm (Fig. 7c). These spectra were characteristic of a *b*-type cytochrome in which the heme is non-covalently attached to the apo-protein (Ozols and Strittmatter, 1964).

As HcpR proteins have been implicated in the response to nitrosative stress, the HcpR1-heme complex was exposed to NO. HcpR1 was supplemented with sub-stoichiometric quantities of hemin and reduced with dithionite in an anaerobic environment (Fig. 8, pale grey line). Gentle bubbling with NO gas resulted in the protein being rapidly decolorized, resulting in a distinct flattening of the absorbance peaks in the 530-560 nm range and also the loss of the Soret peak at 425 nm (Fig. 8, black line). When hemin-supplemented HcpR1 was bubbled with CO gas, the absorbance of the Soret peak increased and the peaks at 530 and 560 nm shifted slightly to 535 nm and 565 nm with a switch in relative peak heights (Fig. 8, medium grey line).

HcpR2 can acquire an iron-sulfur cluster that reacts with O₂ and NO

The *hcpR2* gene was also cloned into the expression plasmid pET21a, and the recombinant plasmid transformed into *E. coli* BL21 (DE3). Highest yields of the His-tagged recombinant HcpR2 were obtained after induction with 0.5 mM IPTG in medium supplemented with 25 mg.l⁻¹ methionine

and 0.1 mM ferrous sulfate. Preparations of HcpR2 were initially pale brown, but this color was lost during subsequent purification and dialysis steps. This suggested that HcpR2 possessed a labile co-factor. Alignment of 12 HcpR2 family proteins revealed the presence of 3 conserved cysteine residues (Cys-25, 117 and 121) and a conserved histidine residue (His-124). There are also four other less well conserved cysteine residues in HcpR2: Cys-8, 22, 41 and 95. Analysis of the primary structure of HcpR2 using the ROBETTA software (Kim et al., 2004) and CprK (PDB: 2h6b) as template predicted that the four fully conserved residues are located close together at the opposite end of the protein to the DNA-binding helix in a three-dimensional model and that the less conserved Cys-22 is located in the same region (Fig. S2; Table S1). This raised the possibility that these amino acid residues could be involved in binding a sensory co-factor that was responsible for the color of HcpR2 during initial purification steps (see above). Anaerobic incubation of HcpR2 with ferrous ions, cysteine and cysteine desulfurase in the presence of a reducing agent converted the colorless aerobically prepared protein into a straw-brown colored protein, indicative of the incorporation of iron-sulfur clusters (Fig. 9a inset 1). The UV-visible spectrum of the reconstituted protein after separation from reaction components by heparin chromatography was similar to other [4Fe-4S] proteins (Fig. 9a: Crack *et al.*, 2012a and b). Total iron analysis for reconstituted HcpR2 protein preparations supported this assignment showing the presence of 3.2 ± 0.1 moles of iron per mole of HcpR2 monomer. The initial coloration of HcpR2-containing fractions during purification, the UV-visible spectrum and iron-content of the reconstituted protein are consistent with HcpR2 existing as a [4Fe-4S] cluster protein under anaerobic conditions, but the possibility that HcpR2 possesses a [3Fe-4S] cluster or a mixture of [4Fe-4S] and [2Fe-2S] cannot be dismissed at this stage (see Table 1 below).

Addition of a two-fold molar excess of O_2 to a solution of reconstituted HcpR2 ($\sim 9.4 \mu\text{M}$ cluster using a typical extinction coefficient of $16,000 \text{ M}^{-1} \text{ cm}^{-1}$) resulted in changes in the UV-visible spectrum consistent with conversion of the [4Fe-4S] cluster to a [2Fe-2S] cluster (Fig. 9a, heavy grey line). Prolonged exposure to air resulted in the degradation of the [2Fe-2S] form, yielding apo-

HcpR2 that lacked absorption bands in the visible region (Fig. 9a, fine grey line). To measure the stoichiometry of the reaction of the HcpR2 [4Fe-4S] cluster with O₂, anaerobic reconstituted protein was titrated with air-saturated buffer. There was a progressive increase in absorbance around 550 nm following sequential additions of air-saturated buffer (~220 μM O₂) to reconstituted HcpR2 (~9.4 μM [4Fe-4S] cluster) and collection of UV-visible spectra after a 10 min reaction period (Fig. 9a). The change in absorbance at 550 nm (ΔA_{550}) was plotted against the ratio of [O₂]:[4Fe-4S]. The intersection of the tangent to the initial slope and the asymptote showed that conversion of the [4Fe-4S] cluster was complete after the addition of 2-3 O₂ molecules per [4Fe-4S] cluster (Fig. 9a inset 2). This stoichiometry is similar to that obtained for the reaction of the [4Fe-4S] cluster of *E. coli* FNR, which was ~87% complete at an O₂ to cluster ratio of 2 (Crack *et al.*, 2008; Zhang *et al.*, 2012). The decrease in ΔA_{550} observed at higher concentrations of O₂ is likely to represent degradation of the [2Fe-2S] form of HcpR2. Thus, it was concluded that like *E. coli* FNR, HcpR2 can acquire an O₂-sensitive [4Fe-4S] cluster that degrades via a [2Fe-2S] cluster in the presence of air to ultimately yield apo-HcpR2 (Green *et al.*, 2009).

Several transcription factors that possess iron-sulfur clusters are known to respond to NO as well as to O₂ (Crack *et al.*, 2012a and b; Green *et al.*, 2013). To determine whether the iron-sulfur clusters of HcpR2 react with NO, reconstituted HcpR2 (~10 μM cluster) was exposed to NO released from the donor molecule proli NONOate. The UV-visible spectrum of NO-treated HcpR2 showed decreased absorbance at wavelengths >425 nm and enhanced absorbance between 300 and 425 nm (Fig. 9b). The presence of shoulders at ~310 nm and ~360 nm after exposure to NO was consistent with formation of a dimeric dinitrosyl-iron-cysteine complex, as previously shown for other iron-sulfur cluster sensor-regulators; however the spectra cross at isosbestic point ~425 nm rather than at the isosbestic points reported for other iron-sulfur proteins (~395 nm) (Cruz-Ramos *et al.*, 2002; Smith *et al.*, 2010; Crack *et al.*, 2011; Crack *et al.*, 2013). The NO-treated HcpR2 protein was subjected to liquid-chromatography mass spectrometry (Fig. 9c). Analysis of the masses suggested the presence of HcpR2 species with [3Fe-4S] and [2Fe-2S] clusters as well as the apo-

protein (Table 1). Several species had masses consistent with modification of both the HcpR2 iron-sulfur cluster (dinitrosyl-iron-cysteine complexes) and the HcpR2 protein itself (*S*-nitrosothiol, intramolecular disulfide bond and persulfide forms). Thus, the species detected were consistent with HcpR2 being an NO-sensitive iron-sulfur protein. Although we cannot exclude the alternative possibility that, like *E. coli* FNR, HcpR2 is an O₂-sensor, we propose that HcpR2 primarily responds to NO. Whichever is correct, it is clear that HcpR1 and HcpR2 use different sensory mechanisms to regulate subsets of genes required for defense against NO-induced nitrosative stress.

DNA-binding by the iron-sulfur cluster form of HcpR2 is impaired by exposure to nitric oxide

Immediately downstream from the *hcpR2* gene is a small intergenic region with a predicted binding site for HcpR2 followed by the small open reading frame designated *ylbA* and then the *hcp* gene (Figs. 1c and 10a). In contrast to the *hcpR1* promoter region, no promoter elements could be identified in the *hcp-ylbA* intergenic region. This intergenic region is only 62 bp in length and the putative HcpR2 binding site, which is an inverted repeat sequence (CCGTAACAATTGTTACGG), overlaps the 3' end of the *hcpR2* gene by six nucleotides. The ability of reconstituted HcpR2 to bind to a DNA fragment containing these sequences was tested by electrophoretic mobility shift assay (EMSA). A single high molecular weight complex formed when HcpR2 was incubated with this DNA fragment, indicating binding of HcpR2 at the *ylbA-hcp* promoter region (Fig. 10b, lanes 1-11). After exposure of reconstituted HcpR2 to NO DNA-binding was impaired (Fig. 10b, lanes 12-14). These data are consistent with a model in which in the absence of nitrosative (or oxidative) stress low constitutive expression of *hcpR2* (Fig. 3a) supplies the cell with apo-HcpR2, which acquires a [4Fe-4S] (two per dimer) and binds at the *ylbA-hcp* intergenic region to repress expression of these genes (Fig. 10c). Nitric oxide (or O₂) is perceived by the HcpR2 iron-sulfur cluster, thereby inhibiting DNA-binding and permitting *ylbA-hcp* expression to counteract the effects of nitrosative (or oxidative) stress.

Discussion

Despite the handicap of our current inability to generate knock-out mutants of *D. desulfuricans*, target DNA sites for both HcpR1 and HcpR2 were predicted and verified. Transcription of *hcpR1* was induced strongly in the presence of NO, consistent with HcpR1 synthesis being regulated in response to nitrosative stress. Initial preparations of HcpR1 protein were colorless, but the presence of conserved residues in HcpR1 homologues, particularly His-93, suggested that the protein might bind heme similar to the distantly related HcpR protein of *P. gingivalis* (Lewis *et al.*, 2012). This heme cofactor of HcpR1 is able to bind CO, which causes a change in the spectrum, and NO, which rapidly decolorized the protein. Spectroscopic analysis was consistent with the proposal that HcpR1 is a heme-containing protein typical of a *b*-type cytochrome that is able to distinguish between CO and NO. However, as hemin binds adventitiously to some proteins (Airola *et al.*, 2010), attempts were made to demonstrate specific binding of hemin to the apoprotein by changing the His-93 codon by site-directed mutagenesis to an alanine codon. In contrast to the high yields of HcpR1 that were easily generated, only small yields or none of the substituted protein were obtained in multiple attempts. The plasmid was sequenced to confirm that no secondary mutations had been inadvertently introduced. Although this indicated that His-93 might be critical for protein folding or stability, it remains possible that heme binds non-specifically to the HcpR1 apoprotein. However, when combined with the spectroscopic analysis, we suggest that this result is consistent with the proposal that HcpR1 is a heme-containing protein typical of a *b*-type cytochrome that can distinguish between CO and NO. If this proposal is correct, we suggest that binding of NO would convert HcpR1 to a form that activates its own transcription. At present it is unknown whether NO induces loss of heme, in which case the apo-HcpR1 would be transcriptionally active, or alternatively whether the NO-bound form of HcpR1 might be the transcription activator.

In contrast to HcpR1, preparations of HcpR2 were initially pale brown, but this color was lost during subsequent purification and dialysis steps. The protein could bind an iron-sulfur cluster

during anaerobic reconstitution with ferrous ions, cysteine and cysteine desulfurase protein. The responses of the reconstituted HcpR2 iron-sulfur cluster to air and NO suggest that HcpR2 might act as a NO- and/or O₂-sensing transcription regulator, but in the context of a role in regulating expression of *hcp* in a nitrate-respiring anaerobe, we propose that HcpR2 primarily responds to NO. Whichever is correct, it is clear that HcpR1 and HcpR2 use different sensory mechanisms to regulate subsets of genes required for defense against NO-induced nitrosative stress.

We speculate that, unlike most other *Desulfovibrio* species that are likely to have two copies of *hcpR* as a result of an ancestral gene duplication event, a lateral gene transfer event has provided *D. desulfuricans* with the distinctive *hcpR2*. It is possible that the *hcpR2* and *hcp* genes were acquired together from another member of the gut microbiome, resulting in the acquisition of an additional protection mechanism. An additional *hcpR* gene would permit specialization of these regulators to fulfill different roles, for example under selective pressure in the gastro-intestinal tract of warm blooded animals where they are exposed to multiple sources of nitrosative stress. In such an environment, although the availability of O₂ and sulfate are limited, other electron acceptors such as nitrate and nitrite are available. The ability to reduce nitrate as an alternative to sulfate would provide both a selective advantage and also an increased requirement for protection against NO generated either by the animal host, or as a side product during nitrate or nitrite reduction to ammonia. The data in figures 3 and 4 show that both *hcpR1* and *hcp* are induced during growth in the presence of nitrate, nitrite or nitric oxide, but *hcpR2* expression is insensitive to the electron acceptor available during growth. Bioinformatic analysis has revealed a clear candidate for an HcpR1 binding site upstream of *hcpR1*, but not in the *hcpR2-ylbA-hcp* region. This suggests that HcpR1 regulates its own synthesis as well as the downstream genes, *wrbA* and *nimA*, but it does not directly regulate expression of *hcpR2* or *hcp*. Conversely, there is a clear candidate for an HcpR2 binding site between *hcpR2* and *ylbA*, but not upstream of *hcpR1*. We therefore speculate that HcpR1 and HcpR2 both respond by different mechanisms to NO and therefore that both proteins are able to sense nitrosative stress and regulate different sub-sets of genes. As more genome

sequences become available, it will be interesting to see whether close homologues of *D. desulfuricans* HcpR2 occur in free-living *Desulfovibrio* strains that are also able to reduce nitrate.

Experimental procedures

Growth of D. desulfuricans

Liquid cultures of *D. desulfuricans* ATCC27774 were grown anaerobically in sterile Postgate media in sealed serum bottles at 30°C (Postgate, 1984). Glycerol stocks of *D. desulfuricans* ATCC27774 that had been stored at -80°C were revived by culturing into the sulfate-containing Postgate B (PgB) medium. Postgate zero medium, lacking terminal electron acceptors, was used to grow *D. desulfuricans* when it was necessary to measure cell densities or harvest cells for RNA purification and SDS-PAGE. Sealed serum bottles of media were flushed with N₂ gas prior to inoculation to provide an anaerobic environment. Generally, cultures of *D. desulfuricans* that had been grown for 48 h, or to stationary phase, were used as inocula.

Preparation of nitric oxide saturated water

Nitric oxide saturated water for use in growth experiments was prepared as described in Vine and Cole (2012). Approximately 5 ml of water was sealed in a glass bijoux bottle and flushed with nitrogen gas for 30-40 min followed by flushing with NO gas for at least 30 min. Nitric oxide saturated water prepared in this way contains 2 mM NO. Nitric oxide saturated water was prepared when required and was introduced to cultures by syringes to prevent exposure to O₂.

RNA purification

Cultures of *D. desulfuricans* were grown as described and 5-15 ml samples were harvested by centrifugation at 4°C. Cell pellets were re-suspended in 3 ml RNeasy lysis buffer (Ambion) and frozen in liquid nitrogen until processed. Total RNA was purified from cells with the QIAGEN RNeasy mini kit according to the manufacturer's instructions with the inclusion of the optional on-column DNaseI digest step to eliminate contaminating DNA. RNA was eluted from the RNeasy spin

columns with 30 μl RNase-free water and stored at -80°C for up to one month. RNA integrity was assessed with a NanoDrop ND1000 Spectrophotometer. Samples with an A_{260}/A_{280} of less than 1.8 and/or an A_{260}/A_{230} outside the range 2.0-2.2 were rejected as were samples with an RNA concentration of less than $200 \text{ ng } \mu\text{l}^{-1}$.

Reverse transcription

RNA was reverse transcribed to cDNA with random hexamer primers using the Tetro cDNA Synthesis kit (BIOLINE) according to the manufacturer's instructions. Each RT-PCR reaction included 2 μg of total RNA. Multiple RT-PCR reactions were prepared from each RNA sample to provide a cDNA pool for each RNA sample.

Quantitative PCR (qPCR)

qPCR was performed on a Stratagene Mxp3005 machine set to detect SYBR green fluorescence. qPCR reactions were made using the Brilliant III Ultra-Fast SYBR® Green QPCR Mastermix kit (Agilent) and using gene specific primers at a final concentration of 400 nM. cDNA template was included at a concentration of 5-50 ng. Primers were designed to measure levels of the *hcpR1* (q0528-F: AACCATCACGAAAGGGATGT; q0528-F: GGAATGCACGAGGTGGAGTA), *hcpR2* (q1827-F: CGTGATGGCCCGTATTGA; q1827-F: TGTTGCGTATGATCTGTGCAT), *hcp* (q1829-F: CCAGGAAACCGTGGGTAAC; q1829-R: AACCAGGCGGTCTATCCTGT) and *polA* (q*polA*-F: CATCTGGACGAAATGTTACC; q*polA*-R: CTGCATGCGTTCAAGAGAAG) transcripts using Primer3 software (Rozen and Skaletsky, 1999). Transcript levels were quantified by the $\Delta\Delta\text{Ct}$ method using the levels of *polA* as a standard (Livak and Schmittgen, 2001). For each growth condition tested in qRT-PCR analyses RNA was prepared from at least three biological replicates and each qPCR was reaction was run in triplicate.

Transcript mapping

To map the *hcpR1* and *hcpR2* operons cDNA was prepared as described above and used as the template for conventional PCR using primers spanning these genomic regions. Primers p0528-F: TACTGCATCCAGGACATTTACC, p0528-R: CATAGTACAATCTCCCGGGCTTTCG, p1827-F: TAACAGAAATTCCCTGGGGC, p1827-R: CATGCGTTCTTCCAGCGTC, p1827cTERM-F: CAACGGAAAAAACATCTCCC, p1827cTERM-R: GGGCAGCGCGGTGGCGTAATCC, Ddes_1828-F: CTTGTTCAAGATGATGCCGTGG, Ddes_1828-R: GATGGACTCTCCGGCCTTGAG, Ddes_0527-F: ATTACGACTGCCTGGCCGTG, Ddes_0527-R: CGGAGTCATCGGGTGGGTAC, Ddes_0526-F2: TGAGGGGCACAAGCTGGACT and Ddes_0526-R: GCATAGCGGACGGCAATGG were used in conjunction with qRT-PCR primers for this analysis.

Protein purification

The coding regions of *hcpR1* and *hcpR2* were amplified by PCR from genomic DNA using primers 0528OE-F2: TTAATCATATGACAAACCGACAATATGCCGCC, 0528OE-R: TTAATGCGGCCGCGCCTTGCGCCCGCAGTTTC, 1827OE-F2: TATATCATATGAATCAGGCCCTGAAAAGCTGCG and 1827OE-R2: TATATGCGGCCGCGGAACAGAATAATCGTAAAATTC. The PCR fragments were cloned into the pET21a expression vector (Novagen) to yield plasmids pETHcpR1 and pETHcpR2. His-tagged HcpR1 and HcpR2 proteins were produced in *E. coli* strain BL21* harboring either of these plasmids. In brief, 10 ml of an overnight culture was used to inoculate 500 ml 2xLB supplemented with 2% glucose and appropriate antibiotics. These cultures were incubated at 30°C with shaking until an OD₆₅₀ of ~0.5 and then supplemented with IPTG to a final concentration of 50 µM for HcpR1 or 500 µM for HcpR2. Cultures were harvested by centrifugation at 8,000 x g for 5 min at 24 h after IPTG addition. Cell pellets were frozen in liquid nitrogen and stored at -80°C.

Frozen cell pellets were supplemented with ice-cold buffer A (50 mM Tris-HCl, pH 8.0; 20 mM imidazole; 400 mM NaCl; 5% glycerol (w/v)) to a final volume of 35 ml and re-suspended by

homogenization. Cells were broken by sonication on ice for 5 x 45 seconds. The lysate was clarified by centrifugation at 35,000 x g for 30 min and then 55,000 x g for 1 h. Proteins were purified using an Äkta Prime HPLC system (GE Healthcare). Clarified lysate was loaded onto a 1 ml nickel-agarose column (GE Healthcare) that had been pre-equilibrated with buffer A. The column was then washed with 20 to 40 ml of buffer A and then 20 ml of buffer A + 10% buffer B (as buffer A but including 500 mM imidazole). Bound proteins were eluted in a 20 ml linear gradient of 10 to 100% buffer B in buffer A.

An additional ion-exchange purification step was necessary to yield pure HcpR2. Fractions containing target protein were pooled and dialyzed against buffer C (50 mM Bis-Tris-HCl, pH 6.5; 250 mM NaCl) The dialyzed sample was then loaded onto a 5 ml SP-FF column (GE Healthcare) that had been pre-equilibrated with buffer C. Proteins were eluted in a linear gradient of 0 to 100% buffer D (as buffer C but containing 1 M NaCl). Fractions containing purified protein were pooled and concentrated on Vivaspin 5 kDa spin columns by centrifugation at 3,200 x g for 1 to 4 h at 4°C.

Polyclonal anti-HcpR antibody production

Purified HcpR proteins were transferred into 50 mM Tris-HCl pH 7.5, 250 mM NaCl, 10% (v/v) glycerol by buffer exchange in a Vivaspin 10 kDa MW cut-off column and concentrated to 5 mg ml⁻¹. Polyclonal antibodies were raised in rabbits by CovalAb UK. The protocol consisted of one injection of 50 µg antigen in 0.5 ml mixed with 0.5 ml complete Freund's adjuvant at day 0 of the immunization protocol. A further two injections were made at 14 and 28 days after the initial injection. Bleeds were taken at day 0 and at 39 and 53 days after the initial immunization. Blood cells were removed and the sera were stored at -20°C until required.

Western blot analysis

HcpR1 protein levels in *D. desulfuricans* were measured by Western blot using anti-HcpR serum. Cultures were grown as described and treated with NO saturated H₂O. Cell pellets were harvested at

intervals and total proteins were resolved by SDS-PAGE. Gels were soaked in blotting buffer (25 mM Tris-HCl; 200 mM glycine; 20% methanol (v/v)) for 5 min and then transferred to a nitrocellulose membrane using a BioRad Semi-dry Transfer System. Following transfer, the membrane was washed with 50 ml of 1 x TBS (50 mM Tris-HCl, pH 8.0; 200 mM NaCl) for 15 min and then blocked with 5% (w/v) blocking powder (BioRad) in 1 x TBS. The membrane was then transferred to a bag containing 30 ml of 2.5% (w/v) blocking powder in 1 x TBS supplemented with 4.5 μ l of anti-HcpR serum. The bag was incubated at room temperature for 2 h with gentle agitation. The membrane was then washed in TBS and incubated with 30 ml 2.5% (w/v) blocking powder in 1 x TBS supplemented with 3 μ l of horseradish peroxidase-conjugated anti-rabbit secondary antibody (GE Healthcare). Finally, the membrane was treated with Amersham ECL Plus Western blotting detection reagents (GE Healthcare) according to the manufacturer's instructions. Western blots were visualized by exposure to Amersham Hyperfilm ECL (GE Healthcare) in a dark room.

HcpR1 electromobility shift assays (EMSAs)

DNA fragments containing promoter proximal DNA sequences were amplified from gDNA by PCR and cloned in pGEM T-easy vector (Promega). Promoter fragments were isolated by restriction digest and purified by electroelution, phenol-chloroform extraction and ethanol precipitation.

Purified DNA fragments were radio-labeled with T4 polynucleotide kinase (NEB) and excess γ 32 P-ATP was removed by passing the reaction mixture through two 200 μ l bed volumes of Sephadex G-50 which had been pre-equilibrated with 1 x TE buffer pH 8.0.

EMSA incubation mixtures were prepared to a final volume of 10 μ l and included: 0.2-1 μ l of radiolabeled DNA fragment, 1 μ l of 10 x Binding buffer (20 mM Tris-HCl, pH 8.0; 100 mM KCl; 2 mM MgCl₂; 10% glycerol (w/v)), 0.5 μ l 4 mM spermidine, 0.5 μ l 400 ng μ l⁻¹ herring sperm DNA, 0.5 μ l 1 mg ml⁻¹ bovine serum albumin and 1 μ l of HcpR1 at an appropriate concentration. EMSA

mixtures were incubated at 25°C for 30 min and then resolved on 6% acrylamide gels prepared with 0.25 x TBE and 0.2% (v/v) glycerol.

Following electrophoresis, gels were fixed in 10% (v/v) acetic acid and 10% (v/v) methanol for 10 min, transferred to 3 mm Whatman filter paper and dried under vacuum. Dried gels were stored in cassettes with a Fuji Imaging Phosphor screen overnight which were then visualized with the Bio-Rad Molecular FX Imager System and QuantityOne software (BioRad).

Spectroscopic measurement of heme binding by HcpR1

UV-visible spectra of HcpR1 were measured in a Jasco V-550 UV/VIS spectrophotometer.

Degassed samples of HcpR1 were sealed in quartz cuvettes and flushed with nitrogen gas. HcpR1 protein (1 ml, 12.5 μ M) was titrated with hemin and spectra were recorded against a cuvette containing buffer and a corresponding quantity of hemin. To assess reactions with NO and CO, HcpR1 was supplemented with sub-stoichiometric quantities of hemin in a sealed cuvette and flushed with nitrogen gas, reduced with dithionite and then a UV-visible spectrum was recorded under anaerobic conditions. Samples were then gently flushed for 1 minute with either CO or NO and additional spectra were recorded.

HcpR2 EMSAs

Biotin labeled fragment (~200 bp) of the short intergenic region between HcpR2 and Ddes-1828 was amplified by PCR and 5'-end biotin p1827cTERM-F 5'CAACGGAAAAACATCTCCC3' and p1827cTERM-R 5'GGGCAGCGCGGTGGCGTAATCC3' primers. The indicated concentrations of HcpR2, reconstituted HcpR2 and reconstituted HcpR2 treated with NO released from the donor molecule Proli NONOate under anaerobic conditions were incubated with ~20 fmol of 5'-end biotin labeled DNA in KG buffer (2x buffer: 200 mM potassium glutamate, 50 M Tris-acetate (pH 7.6), 20 mM magnesium acetate, 100 μ g ml⁻¹ BSA, 20 mM DTT) for 30 min at room temperature. Loading

buffer 6x (15% (w/v) Ficoll 400, 0.25% (w/v) Bromophenol blue, 0.25 % (w/v) Xylene cyanol in 1x TBE buffer) was added to the samples prior loading onto 7.5% polyacrylamide gels buffered with 0.25x TBE and 5% (w/v) glycerol. The gels were pre-run for 60 min at 100 V and the protein-DNA complexes were separated for 2 h at 100 V. The DNA was transferred to positively-charged nylon membrane (GE Healthcare) using cooled 0.5x TBE buffer at 380 mA for 30 min and cross-linked by exposure to UV light (120 mJ cm⁻² for 60 s). Chemiluminescent Nucleic Acid Detection Module kit (Thermo Scientific) was used to detect biotin-labeled DNA according to manufacturer's instructions.

Anaerobic reconstitution of iron-sulfur clusters of HcpR2

All of the reagents, including the protein solutions, used in the reconstitution of the apo-HcpR2 iron-sulfur cluster were made anaerobic by incubation in a DW Scientific Anaerobic Workstation (Don Whitley Scientific Ltd., Shipley, UK). Protein samples (typically 2.5 mg ml⁻¹; 0.5-1.0 ml) were incubated with L-cysteine (0.5 mM), ammonium ferrous sulfate (0.2 mM), dithiothreitol (12.5 mM) and the cysteine desulfurase NifS (~0.3 μM) under anaerobic conditions for 16 h at 25°C. Heparin chromatography was used to separate reconstituted HcpR2 from other reaction components (Crack *et al.*, 2008). All of the following procedures were carried out in the anaerobic workstation. An aliquot (1 ml) of reconstituted HcpR2 protein was diluted 2-fold using anaerobic 25 mM Tris-HCl buffer (pH 7.4). The diluted sample was applied to a 1 ml HiTrap heparin column (GE Healthcare) equilibrated with 25 mM Tris-HCl buffer (pH 7.4). The heparin column was washed with 3-column volumes of equilibration buffer to remove low molecular weight reaction components. The reconstituted HcpR2 protein was then eluted by applying 25 mM Tris-HCl (pH 7.4) buffer containing 0.5 M NaCl from the bottom of the column to minimize dilution of the protein. The colored eluate was collected by hand into microcentrifuge tubes. Colored fractions could then be transferred to cuvettes, which were closed with a screw cap fitted with a septum made

from rubber and coated with Teflon, before removing reconstituted protein from the anaerobic workstation.

Iron assay

The protein concentration of the reconstituted and heparin purified HcpR2 protein samples was measured using the Bio-Rad protein assay (Bradford, 1976). Samples were then boiled in 1% (w/v) trichloroacetic acid for 5 min. After centrifugation in a bench top microcentrifuge (13,000 rpm for 5 min) the supernatant was removed and retained. The amount of iron released was measured by incubation of supernatant (480 μ l) with saturated sodium acetate (400 μ l), 10% (w/v) bathophenanthroline sulfonic acid (30 μ l) and 20% (w/v) freshly prepared sodium ascorbate (90 μ l). After adding sodium ascorbate all the iron present in the sample was reduced to the ferrous state and formed a complex with the bathophenanthroline, resulting in a red coloration. Absorbance of the ferrous-bathophenanthroline complex was then measured at 535 nm and compared to a standard curve prepared using dilutions of an iron standard solution (17.86 mM; Alfa Aesar).

Sensitivity of the HcpR2 iron-sulfur cluster to oxygen

The UV-visible spectrum (250–750 nm) of the reconstituted HcpR2 protein was recorded under anaerobic conditions using a Cary Eclipse Spectrophotometer (Agilent). The reaction of the iron-sulfur cluster with O₂ was measured by titrating the protein with increasing volumes of air-saturated (~220 μ M O₂) buffer (25 mM Tris, pH 7.4 containing 0.5 M NaCl). After each addition the reaction was allowed to proceed for 10 min at room temperature before UV-visible spectra were obtained (Crack *et al.*, 2008).

Reaction of HcpR2 iron-sulfur clusters with nitric oxide

Reconstituted HcpR2 (1 ml; ~10 μ M cluster) was transferred to a cuvette under anaerobic conditions. After obtaining UV-visible spectra up to 400 μ M NO (final concentration) was introduced into the cuvette by injection of aliquots of proli NONOate (Cayman Chemicals; 500 μ M

in 10 mM NaOH). After reaction for 30 min the UV-visible spectrum of the NO-treated protein was obtained.

Liquid chromatography-mass spectrometry of reconstituted HcpR2

An aliquot of NO-treated (~400 μM) reconstituted HcpR2 (initial cluster concentration 10 μM) was injected onto an Extended C18 column (2.1 mm x 50 mm; Agilent) equilibrated with 0.1% (v/v) formic acid. Bound protein was eluted (0.4 ml min⁻¹) with a linear gradient of acetonitrile containing 0.1% (v/v) formic acid (5%-95% in 10 min) using an Agilent 1260 Infinity Liquid Chromatography instrument. An Agilent 6530 Q-ToF mass spectrometer operating in ESI positive mode, with drying gas temperature 350°C, flow rate 1L/min, nebuliser 45 psig, and capillary voltage 4000 V.

Protein assays

The Bio-Rad reagent was used to estimate the concentration of proteins (Bradford, 1976). The concentration of HcpR2 protein was also calculated using the HcpR2 extinction coefficient (9315 M⁻¹ cm⁻¹) calculated using the Expasy Protparam tool (Gasteiger *et al.*, 2003).

Bioinformatics and data analysis

DNA and protein sequences were analyzed with a range of on-line tools. Putative RNAP -10 and -35 sequences were identified using the Softberry BPROM tool (Softberry Inc., Mount Kisco, NY, USA). CRP binding sites were identified in promoters and whole genome sequences using Virtual Footprint and PRODORIC (Münch *et al.*, 2005). Genome sequences were scanned for custom sequences using the EMBOSS program fuzznuc (Rice *et al.*, 2000). Groups of DNA or protein sequences were scanned for conserved motifs using the MEME tool (Bailey *et al.*, 2015). Multiple alignments of DNA sequences and proteins were made using ClustalW (Larkin *et al.*, 2007). Protein structure homology searches were made using the PHYRE2 tool (Kelley *et al.* 2015).

Statistical significance of data was assessed using the paired samples t-test in Microsoft Excel. The p values indicated data significantly different where $p \leq 0.050$. For qRT-PCR assays the p values were determined from the ΔC_t values.

Acknowledgements

The authors are grateful to Dr Angeliki Marietou for assistance with growing *Desulfovibrio*, to Dr Kerry Hollands for advice on EMSAs and Simon Thorpe for assistance with mass spectrometry. ITC was funded by The University of Birmingham, UK, SAI was funded by a scholarship from the Higher Committee for Education and Development in Iraq and JG is grateful for support from the Biotechnology and Biological Science Research Council UK (BB/L008114/1). Authors declare no conflict of interest.

References

- Airola, M.V., Du, J., Dawson, J.H. and Crane, B.R. (2010) Heme binding to the mammalian circadian clock protein period 2 is nonspecific. *Biochemistry* **49**: 4327-4338
- Bailey, T.L., Johnson, J., Grant, C.E., and Noble, W.S. (2015) The MEME Suite. *Nucl Acids Res* gkv416.
- Bordoli, L., Kiefer, F., Arnold, K., Benkert, P., Battey, J., and Schwede, T. (2009) Protein structure homology modelling using SWISS-MODEL workspace. *Nat Protoc* **4**: 1.
- Boutrin, M.-C., Wang, C., Aruni, W., Li, X., and Fletcher, H.M. (2012) Nitric oxide stress resistance in *Porphyromonas gingivalis* is mediated by a putative hydroxylamine reductase. *J Bacteriol* **194**: 1582–1592.
- Bradford, M.M. (1976) A rapid and sensitive method for the quantitation of microgram quantities of protein utilizing the principle of protein-dye binding. *Anal Biochem* **72**: 248-254.

Cadby, I.T., Busby, S.J.W., and Cole, J.A. (2011) An HcpR homologue from *Desulfovibrio desulfuricans* and its possible role in nitrate reduction and nitrosative stress. *Biochem Soc Trans* **39**: 224.

Chakravarti, R., Aulak, K.S., Fox, P.L., and Stuehr, D.J. (2010) GAPDH regulates cellular heme insertion into inducible nitric oxide synthase. *Proc Natl Acad Sci USA* **107**: 18004-18009.

Chismon, D., Browning, D., Farrant, G., and Busby, S. (2010) Unusual organization, complexity and redundancy at the *Escherichia coli* *hcp-hcr* operon promoter. *Biochem J* **430**: 61-68.

Constantinidou, C.C., Hobman, J.L., Patel, M.D., Penn, C.W., Cole, J.A., and Overton, T.W. (2006) A reassessment of the fumarate and nitrate reduction regulon and transcriptomic analysis of the effects of nitrate, nitrite, NarXL and NarQP as *Escherichia coli* adapts from aerobic to anaerobic growth. *J Biol Chem* **281**: 4802-4808.

Crack, J.C., Le Brun, N.E., Thomson, A.J., Green, J., and Jervis, A.J. (2008) Reactions of nitric oxide and oxygen with the regulator of fumarate and nitrate reduction, a global transcriptional regulator, during anaerobic growth of *Escherichia coli*. *Meth Enzymol* **437**: 191-209.

Crack, J.C., Green, J., Hutchings, M.I., Thomson, A.J., and Le Brun, N.E. (2012a) Bacterial iron-sulfur regulatory proteins as biological sensor-switches. *Antioxid Redox Signal* **17**: 1215-1231.

Crack, J.C., Green, J., Thomson, A.J., and Le Brun, N.E. (2012b) Iron-sulfur cluster sensor-regulators. *Curr Opin Chem Biol* **16**: 35-44.

Crack, J.C., Smith, L.J., Stapleton, M.R., Peck, J., Watmough, N.J., Buttner, M.J., Buxton, R.S., Green, J., Oganessian, V.S., Thomson, A.J., and Le Brun, N.E. (2011) Mechanistic insight into the nitrosylation of the [4Fe-4S] cluster of WhiB-like proteins. *J Am Chem Soc* **133**: 1112-1121.

Crack, J.C., Stapleton, M.R., Green, J., Thomson, A.J., Le Brun, N.E. (2013) Mechanism of [4Fe-4S](Cys)₄ cluster nitrosylation is conserved among NO-responsive regulators. *J Biol Chem* **288**: 11492-11502.

Cruz-Ramos, H., Crack, J., Wu, G., Hughes, M.N., Scott, C., Thomson, A.J., Green, J., and Poole, R.K. (2002) NO sensing by FNR: regulation of the *Escherichia coli* NO-detoxifying flavohaemoglobin, Hmp. *The EMBO J* **21**: 3235-3244.

da Silva, S.M., Amaral, C., Neves, S.S., Santos, C., Pimentel, C., and Rodrigues-Pousada, C. (2015) An HcpR paralogue of *Desulfovibrio gigas* provides protection against nitrosative stress. *FEBS Open Bio* **5**: 594-604.

Ebright, R.H. (1993) Transcription activation at class I CAP-dependent promoters. *Mol Microbiol* **8**: 797-802.

Figueiredo, M.C.O., Lobo, S.A.L., Sousa, S.H., Pereira F.P., Wall, J.D., Nobre, L.S., and Saraiva, L.M. (2013) Hybrid cluster proteins and flavodiiron proteins afford protection to *Desulfovibrio vulgaris* upon macrophage infection. *J Bacteriol* **195**: 2684–2690.

Fileenko, N., Spiro, S., Browning, D.F., Squire, D., Overton, T.W., Cole, J., and Constantinidou, C. (2007) The NsrR regulon of *Escherichia coli* K-12 includes genes encoding the hybrid cluster protein and the periplasmic, respiratory nitrite reductase. *J Bacteriol* **189**: 4410-4417.

Fox, J.G., Dewhirst, F.E., Fraser, J., Shames, B., and Murphy, J.C. (1994) intracellular *Campylobacter*-like organism from ferrets and hamsters with proliferative bowel disease is a *Desulfovibrio* sp. *J. Clin. Microbiol.* **32**: 1229-1237.

Gardner, A.M., and Gardner, P.R. (2002) Flavohemoglobin detoxifies nitric oxide in aerobic, but not anaerobic, *Escherichia coli* evidence for a novel inducible anaerobic nitric oxide-scavenging activity. *J Biol Chem* **277**: 8166-8171.

- Gasteiger E., Gattiker A., Hoogland C., Ivanyi I., Appel R.D., and Bairoch A. (2003) ExPASy: the proteomics server for in-depth protein knowledge and analysis. *Nucl Acid Res* **31**: 3784-3788.
- Gomes, C.M., Giuffre, A., Forte, E., Vicente, J.B., Saraiva, L.M., Brunori, M., and Teixeira, M. (2002) A novel type of nitric-oxide reductase *Escherichia coli* flavorubredoxin. *J Biol Chem* **277**: 25273-25276.
- Green J., Crack J.C., Thomson A.J., and LeBrun N.E. (2009) Bacterial sensors of oxygen. *Curr Opin Microbiol* **12**: 145-151.
- Green, J., Rolfe, M.D., and Smith, L.J. (2013) Transcriptional regulation of bacterial virulence gene expression by molecular oxygen and nitric oxide. *Virulence* **5** 1-16.
- Jia, W., Faulkner, M., Cadby, I., and Cole, J. (2013) Why was *Desulfovibrio fairfieldensis* not found in faecal DNA from patients with gastric disease? *Path. Dis.* **67**: 3.
- Jia, W., Whitehead, R.N., Griffiths, L., Dawson, C., Bai, H., Waring, R.H., Ramsden, D.B., Hunter, J.O., Cauchi, M., Bessant, C., Fowler, D.P., Walton, C., Turner, C., and Cole, J.A. (2012) Diversity and distribution of sulphate-reducing bacteria in human faeces from healthy subjects and patients with inflammatory bowel disease. *FEMS Immunol Med Microbiol* **65**: 55-68.
- Johnson, S., Lin, S., Lee, P., Caffrey, S.M., Wildschut, J., Voordouw, J.K., *et al.* (2009) A genomic island of the sulfate-reducing bacterium *Desulfovibrio vulgaris* Hildenborough promotes survival under stress conditions while decreasing the efficiency of anaerobic growth. *Environ Microbiol* **11**: 981-991.
- Keith, S.M., and Herbert, R.A. (1983) Dissimilatory nitrate reduction by *Desulfovibrio*. *FEMS Microbiol Lett* **18**: 55-59.
- Kelley, L.A., Mezulis, S., Yates, C.M., Wass, M.N., and Sternberg, M.J. (2015) The Phyre2 web portal for protein modeling, prediction and analysis. *Nat Protoc* **10**: 845-858.

- Kim, D.E., Chivian, D., and Baker, D. (2004) Protein structure prediction and analysis using the ROBETTA server. *Nucl Acids Res* **32**: W526-W531.
- Larkin, M.A., Blackshields, G., Brown, N.P., Chenna, R., McGettigan, P.A., McWilliam, H., Valentin, F., Wallace, I.M., Wilm, A., Lopez, R., and Thompson, J.D. (2007) Clustal W and Clustal X version 2.0. *Bioinformatics*, **23**: 2947-2948.
- Larsen, R.W., MacLeod, J., Shiemke, A.K., Musser, S. ., Nguyen, H.H., Chan, S.I., Nunez, D.J. and Ondrias, M.R. (1992). Spectroscopic characterization of heme a reconstituted myoglobin. *J Inorg. Biochem* **48**: 21-31.
- Lewis, J.P., Yanamandra, S.S., and Anaya-Bergman, C. (2012) HcpR of *Porphyromonas gingivalis* is required for growth under nitrosative stress and survival within host cells. *Infect Immun* **80**: 3319-3331.
- Livak, K.J., and Schmittgen, T.D. (2001) Analysis of relative gene expression data using real-time quantitative PCR and the 2⁻ ΔΔCT method. *Methods* **25**: 402-408.
- Loubinoux, J., Mory, F., Pereira, I.A.C, and Le Four, A.E. (2000) Bacteremia caused by a strain of *Desulfovibrio* related to the provisionally named *Desulfovibrio fairfieldensis*. *J Clin Microbiol* **38**: 931-934.
- Loubinoux, J., Bonowicki, J.-P., Pereira, I.A.C., Mougénel, J.-L., and Le Faou, A.E. (2002) Sulfate-reducing bacteria in human feces and their association with inflammatory bowel diseases. *FEMS Microbiol Ecol* **40**: 107-122.
- Marietou, A., Griffiths, L., and Cole, J. (2009) Preferential reduction of the thermodynamically less favorable electron acceptor, sulfate, by a nitrate reducing strain of the sulfate reducing bacterium, *Desulfovibrio desulfuricans* 27774. *J Bacteriol* **191**: 882-889.
- McCready, R.G.L., Gould, W.D., and Cook, F.D. (1983) Respiratory nitrate reduction by *Desulfovibrio* sp. *Arch Microbiol* **135**: 182-185.
- Mitchell, G.J., Jones, J.G., and Cole, J.A. (1985) Distribution and regulation of nitrate and nitrite reduction by *Desulfovibrio* and *Desulfotomaculum* species. *Arch Microbiol* **144**: 35-40.

Moura, I., Bursakov, S., Costa, C. and Moura, J.J.G. (1997) Nitrate and nitrite utilization in sulphate-reducing bacteria. *Anaerobe* **3**: 279-290.

Münch, R., Hiller, K., Grote, A., Scheer, M., Klein, J., Schobert, M., and Jahn, D. (2005) Virtual Footprint and PRODORIC: an integrative framework for regulon prediction in prokaryotes. *Bioinformatics* **21**: 4187-4189.

Ozols, J., and Strittmatter, P. (1964) The interaction of porphyrins and metalloporphyrins with apocytochrome *b5*. *J Biol Chem* **239**: 1018-1023.

Poock, S.R., Leach, E.R., Moir, J.W., Cole, J.A., and Richardson, D.J. (2002) Respiratory detoxification of nitric oxide by the cytochrome *c* nitrite reductase of *Escherichia coli*. *J Biol Chem* **277**: 23664-23669.

Postgate, J.R. (1984) Genus *Desulfovibrio* Desulfovibrio Kluyver and van Niel 1936, 397^{AL}. In N. L. Krieg and J. G. Holt (ed.), *Bergey's manual of systematic bacteriology*, vol. 1, p. 666-672. The Williams and Wilkins Co., Baltimore, MD.

Rabus, R., Venceslau, S.S., Wöhlbrand, L., Voordouw, G., Wall, J.D.I., and Pereira, I.A.C. (2015) A post-genomic view of the ecophysiology, catabolism and biotechnological relevance of sulphate-reducing prokaryotes. *Adv Microb Physiol* **66**: 55-321.

Rice, P., Longden, I., and Bleasby, A. (2000) EMBOSS: the European molecular biology open software suite. *Trends Genet* **16**: 276-277.

Rodionov, D.A., Dubchak, I.L., Arkin, A.P., Alm, E.J., and Gelfand, M.S. (2004) Reconstruction of regulatory and metabolic pathways in metal-reducing delta proteobacteria. *Genome Biol* **5**: R90.

Rodionov, D.A., Dubchak, I.L., Arkin, A.P., Alm, E.J., and Gelfand, M.S. (2005) Dissimilatory metabolism of nitrogen oxides in bacteria: comparative reconstruction of transcriptional networks. *PLoS Comp Biol* **1**: e55.

- Rozen, S., and Skaletsky, H. (1999). Primer3 on the WWW for general users and for biologist programmers. In *Bioinformatics methods and protocols* (pp. 365-386). Humana Press.
- Schneider, S., Marles-Wright, J., Sharp, K.H., and Paoli, M. (2007) Diversity and conservation of interactions for binding heme in *b*-type heme proteins. *Nat Prod Rep* **24**: 621-630.
- Senez, J.C., and Pichinoty, F. (1958) Réduction de l'hydroxylamine liée à l'activité de l'hydrogénase de *desulfovibrio desulfuricans*: II. Nature du système enzymatique et du transporteur d'électrons intervenant dans la réaction. *Biochim Biophys Acta* **28**: 355-369.
- Seth, D., Hausladen, A., Wang, J-Y., and Stamler, J.S. (2012) Endogenous protein S-nitrosylation in *E. coli*: regulation by OxyR. *Science* **336**: 470-473.
- Smith, L.J., Stapleton, M.R., Fullstone, G.J., Crack, J.C., Thomson, A.J., Le Brun, N.E., Hunt, D.M., Harvey, E., Adinolfi, S., Buxton, R.S., and Green, J. (2010) *Mycobacterium tuberculosis* WhiB1 is an essential DNA-binding protein with a nitric oxide-sensitive iron-sulfur cluster. *Biochem J* **432**: 417-427.
- van den Berg, W.M., Hagen, W.R., and van Dongen, W.M.A.M. (2000) The hybrid cluster ("prismane protein") from *Escherichia coli*. *Eur J Biochem* **267**: 666-676.
- van Wonderen, J.H., Burlat, B., Richardson, D.J., Cheesman, M.R. and Butt, J.N. (2008) The nitric oxide reductase activity of cytochrome *c* nitrite reductase from *Escherichia coli*. *J Biol Chem* **283**: 9587-9594.
- Vine, C.E., and Cole, J.A. (2011) Unresolved sources, sinks and pathways for the recovery of enteric bacteria from nitrosative stress. *FEMS Microbiol Lett* **325**: 99-107.
- Wang, J., Vine, C. E., Balasiny, B. K., Rizk, J., Bradley, C. L., Tinajero-Trejo, M., Poole, R. K., Bergaust, L. L., Bakken, L. R. and Cole, J. A. (2016) The roles of the hybrid cluster protein,

Hcp, and its reductase, Hcr, in high affinity nitric oxide reduction that protects anaerobic cultures of *Escherichia coli* against nitrosative stress. *Mol Microbiol* **100**: 877-892.

Widdel, F., and Pfennig, N. (1982). Studies of dissimilatory sulfate-reducing bacteria that decompose fatty acids. II. Incomplete oxidation of propionate by *Desulfobulbus propionicus* gen. nov., sp. nov. *Arch Microbiol* **131**: 360-365.

Yurkiw, M.A., Voordouw, J., and Voordouw, G. (2012) Contribution of rubredoxin: oxygen oxidoreductases and hybrid cluster proteins of *Desulfovibrio vulgaris* Hildenborough to survival under oxygen and nitrite stress. *Environ Microbiol* **14**: 2711-2725.

Zhang, B., Crack, J.C., Subramanian, S., Green, J., Thomson, A.J., Le Brun, N.E., and Johnson, M.K. (2012) Reversible cycling between cysteine persulfide-ligated [2Fe-2S] and cysteine-ligated [4Fe-4S] clusters in the FNR regulatory protein. *Proc Natl Acad Sci USA* **109**: 15734-15739.

Zhou, A., Chen, Y.I., Zane, G.M., He, Z., Hemme, C.L., Joachimiak, M.P., Baumohl, J.K., He, Q., Fields, M.W., Arkin, P., Wall, J.D., and Hazen, T.C. (2012) Functional characterization of Crp/Fnr-type global transcriptional regulators in *Desulfovibrio vulgaris* Hildenborough. *Appl Environ Microbiol* **78**: 1168–1177.

Table 1. Liquid chromatography-mass spectrometry analysis of reconstituted HcpR2 treated with nitric oxide

Measured mass (Da) ^a	Additional mass (Da) ^b	Modification ^c	Expected mass change associated with modification(s) (Da)
26,732.91	-4.49	2 intramolecular disulfide bonds	-4.04
26,762.86	25.46	2 intramolecular disulfide bonds, 1 <i>S</i> -nitrosothiol	24.96
26,780.40	43.09	2 intramolecular disulfide bonds, 1 cysteine persulfide, 1 MetSO	44.01
26,794.65	57.52	2 <i>S</i> -nitrosothiol	58.04
26,812.92	75.52	2 intramolecular disulfide bonds, 2 cysteine persulfides, 1 MetSO	76.09
26,828.17	90.77	2 intramolecular disulfide bonds, 3 cysteine persulfides	92.23
26,847.27	109.87	2 intramolecular disulfide bonds, 1 monomeric dinitrosyl-iron-cysteine complex	109.81
26,861.25	123.85	2 intramolecular disulfide bonds, 4 cysteine persulfides	124.22
26,878.80	141.4	1 intramolecular disulfide bond, 1 monomeric dinitrosyl-iron-cysteine complex, 1 <i>S</i> -nitrosothiol	140.83
26,910.25	172.85	[2Fe2S] cluster	171.78
26,931.84	194.44	2 intramolecular disulfide bonds, 1 dimeric dinitrosyl-iron-cysteine complex with 3 NO ligands	195.56
26,962.10	224.47	2 intramolecular disulfide bonds, dimeric dinitrosyl-iron-cysteine complex	225.56
26,993.46	256.06	1 intramolecular disulfide bond, 1 dimeric dinitrosyl-iron-cysteine complex, 1 <i>S</i> -nitrosothiol	256.66
27,026.78	289.38	[3Fe4S] cluster	289.4

^a Mass of species detected (Fig. 8c).

^b Additional mass relative to apo-HcpR2 (26,737.4 Da).

^c Possible modifications of HcpR2 that are consistent with observed mass increases (MetSO, oxidized methionine).

Figure legends

Fig. 1. The genomic loci of *hcpR1* and *hcpR2* in *D. desulfuricans* and closely related species.

Arrows represent putative genes. Matching colors indicate conserved genes.

Fig. 2. Transcript mapping of the *hcpR1* and *hcpR2* loci. (a) Primers were designed to amplify DNA fragments spanning the coding regions of the *hcpR1* and *hcpR2* loci. Additional primers, specific to DNA sequences upstream of the putative *hcpR1* and *hcpR2* promoters, were included.

Combinations of these primers were expected to generate PCR fragments of different sizes and were allocated a letter A-P. These are represented in the cartoon. (b) Primer combinations were

used for a series of PCRs using either *D. desulfuricans* gDNA or cDNA as template. Negative control PCRs using no template DNA were also included. PCR products were resolved by agarose gel electrophoresis. Bioline Hyperladder II was used as a standard on the gel to assess PCR

fragment sizes. Fragments of corresponding sizes were generated for all primer combinations when gDNA was used as the PCR template. Fragments were generated for all primer combinations except those utilizing the *hcpR1* or *hcpR2* promoter primers when cDNA from *D. desulfuricans* was used as the template. No fragments were generated when no template was used (data not shown).

Fig. 3. Effect of the terminal electron acceptor during growth on expression of *hcpR1* and *hcpR2* genes. RNA was purified from samples of early exponential phase cultures of *D. desulfuricans* 27774 grown in media containing 7.5 mM nitrate (unshaded bars) or sulfate (dark grey shading) or 2.5 mM nitrite (pale grey shading) as the only terminal electron acceptor. Transcript levels were determined by qRT-PCR normalized against levels of *polA* mRNA. Expression levels were derived from three biological replicates and triplicate qPCR reactions. Expression levels were normalized to those of the sulfate grown culture. Stars indicate data derived from ΔC_t values significantly different to those for sulfate-grown cultures ($p < 0.05$).

Fig. 4. RT-qPCR of *hcpR* genes in *D. desulfuricans*. Cells were grown on medium containing 15 mM sulfate as the sole terminal electron acceptor. Once cultures reached an OD_{600} of ~ 0.3 they

were treated with 7.5 μM NO. After 20 h the cells were harvested and used for RNA isolation. Total RNA was reverse-transcribed with random hexamers and the resulting cDNA was used for qPCR

analysis. Transcript levels were normalized against *polA* levels and expression levels are derived from three biological replicates and are normalized to those given by untreated sulfate grown cells.

(a) levels of *hcpR1* and *hcpR2* mRNA; (b) levels of *hcp* mRNA. Stars indicate data derived from ΔCt values significantly different to that for untreated cultures.

Fig. 5. The effects of exogenous NO on levels of HcpR1 synthesis. (a) Sulfate grown cells were used to inoculate cultures supplemented with 7.5 mM sulfate and cell densities were monitored over time by measuring OD_{600} . After 18 h the cultures were treated with a low 5 μM dose of NO (black diamonds), a high 25 μM dose of NO (grey triangles) or no treatment (grey circles). Results are the average of three separate biological replicates and error bars indicate standard deviations. (b)

Standardized protein samples were prepared from cells harvested at 0, 4, 24 and 50 h post-treatment. Proteins were resolved by SDS-PAGE and used for Western blot analysis using anti-HcpR1 antibodies. Each track was loaded with 3 μg of soluble cell protein.

Fig. 6. HcpR1 is a DNA-binding protein. (a) A potential HcpR1 DNA target site was identified upstream of the *hcpR1* gene. Putative -10 and -35 promoter elements and ribosome binding site (RBS) were also identified. (b) Binding of HcpR1 to a DNA fragment containing the predicted HcpR1 site was assessed by EMSA. ^{32}P -labelled *hcpR1* promoter DNA fragment was incubated with increasing concentrations of HcpR1 and then resolved by non-denaturing electrophoresis. Herring sperm DNA was also included in the incubation mixtures to act as non-specific competitor DNA. HcpR1 was included in the incubations at 0, 25, 50, 100 and 200 nM. Free DNA and HcpR1-DNA complexes are marked with arrows. Note that although the DNA fragment used in these experiments was purified and extracted from a polyacrylamide gel, it was still contaminated by a larger fragment (the upper band in track 1 of the gel in Fig. 6(b)).

Fig. 7. Binding of hemin to HcpR1. (a) HcpR1 (12.5 μM) was titrated with hemin and UV-visible spectra were recorded against a cuvette containing buffer and a corresponding quantity of hemin.

Addition of hemin to HcpR1 resulted in an increase in absorbance at 415 nm, 532 nm and 565 nm, indicating that hemin was bound by HcpR1. Inset highlights the increase in absorbance around 450-600 nm of HcpR1 on addition of hemin. (b) Absorbance at 415 nm, normalized to the absorbance at 280 nm (Chakravarti *et al.*, 2010; Larson *et al.*, 2012), was plotted against the molar ratio of hemin:HcpR1. The plot indicates that HcpR1 was saturated with hemin at a molar ratio of approximately 1.2:1 (hemin:HcpR1) suggesting that HcpR1 binds hemin with a stoichiometry of 1:1. (c) The addition of dithionite to hemin supplemented HcpR1 resulted in a change in the absorbance profile with the peaks shifting to 425 nm, 530 nm and 560 nm. Reduced HcpR1 hemin (solid black line) and non-reduced HcpR1 hemin (broken line).

Fig. 8. Binding of NO and CO by the HcpR1 ligated Fe^{2+} -heme. HcpR1 (30 μM) was supplemented with a sub-stoichiometric (10 μM) quantity of hemin, reduced with dithionite and then a UV-visible spectrum was recorded under anaerobic conditions. Samples were then gently flushed for 1 minute with either CO or NO and additional spectra were recorded. Treatment with CO resulted in a change in the absorbance profile with peaks shifting to 418 nm, 537 nm and 565 nm. Treatment with NO resulted in a loss of absorbance peaks typical for protein-ligated heme suggesting that heme is lost from HcpR1 when bound to NO.

Fig. 9. Reconstituted HcpR2 has spectral properties consistent with the presence of an oxygen- and nitric oxide sensitive iron-sulfur cluster. (a) Apo-HcpR2 was reconstituted as described in *Experimental procedures* (inset 1). The UV-visible spectrum (heavy black line; $\sim 9.4 \mu\text{M}$ cluster) was typical of a [4Fe-4S] protein. Reconstituted HcpR2 was titrated with aliquots of air-saturated buffer (220 μM O_2 at room temperature) such that the final concentrations of O_2 were 0.0, 4.3, 8.5, 16.3, 30.3, 53.3, 85.85, 107.75, and 123.50 μM . After each addition the reaction was incubated at room temperature for 10 min before measurement of further spectra (fine black lines). The major

change in absorbance associated with conversion of the [4Fe-4S] form (heavy black line) to the [2Fe-2S] form (heavy grey line) is indicated by the arrow. Prolonged air-exposure resulted in the formation of apo-HcpR2 (fine grey line). The changes in absorbance at 550 nm ($\Delta A_{550\text{ nm}}$), representing the appearance of the [2Fe-2S] cluster, are plotted against the ratio of $[O_2]:[4Fe-4S]$ in inset 2. The lines join the tangent to the initial slope to the asymptote of the curve; the dashed line indicates the likely stoichiometry of the reaction. (b) Spectra of reconstituted HcpR2 ($\sim 10\ \mu\text{M}$ cluster) under anaerobic conditions before (black line) and after 30 min incubation at room temperature in the presence of $400\ \mu\text{M}$ NO (grey line). (c) Detection of nitrosylated iron-sulfur clusters and nitrosated protein after treatment of reconstituted HcpR2 (initially $\sim 10\ \mu\text{M}$ cluster) with NO ($\sim 400\ \mu\text{M}$). Samples were analyzed by liquid chromatography-mass spectrometry as described in *Experimental procedures*. The HcpR2 species corresponding to 14 peaks in the mass spectrum are listed in Table 1.

Fig. 10. DNA-binding by reconstituted HcpR2 is impaired by exposure to nitric oxide. (a) A candidate HcpR2 DNA target site was identified in the intergenic region between, and slightly overlapping with, *hcpR2* and the downstream *ylbA-hcp* genes. Although a putative RBS binding site was identified, no obvious promoter elements were found. Binding of HcpR2 to a DNA fragment containing this sequence was assessed by EMSA. (b) Effect of the HcpR2 iron-sulfur cluster and NO on DNA-binding. DNA from the intergenic region of *hcpR2* and *ylbA* containing the predicted HcpR2 binding site (shown in Fig. 10a) was incubated with different concentrations of HcpR2. HcpR2-DNA complexes were resolved by non-denaturing electrophoresis under anaerobic conditions. The HcpR2 concentrations were calculated for a dimer, based on the elution of HcpR2 in size exclusion chromatography experiments. Left panel: concentrations of reconstituted HcpR2 were (nM): lane 1, 0; lane 2, 50; lane 3, 100; lane 4, 200 nM; lane 5, 400; lane 6, 500; lane 7, 800; lane 8, 1000; lane 9, 1200; lane 10, 1400; lane 11, 1500. Middle panel: lane 12, no HcpR; lane 13 reconstituted HcpR2 (1000 nM); and lane 14, HcpR2 (1000 nM) that had been exposed to NO. Right panel: lane 15 no HcpR2; lane 16, reconstituted HcpR2 (1500 nM); and lane 17,

unreconstituted apo-HcpR2 (1500 nM). Free DNA and HcpR2-DNA complexes are marked with arrows. (c) Model of the regulation of *hcpR2-yblA-hcp* operon by HcpR2 in response to NO- and

O₂-mediated stress. It is suggested that the *hcpR2* gene undergoes low level constitutive transcription. Translation of *hcpR2* mRNA generates apo-HcpR2, which incorporates one [4Fe-4S] cluster per protomer. The [4Fe-4S] form of HcpR2 binds at an inverted repeat DNA sequence (CCGTAACAATTGTTACGG) located in the *hcpR2-yblA* intergenic region to repress expression of *yblA-hcp*. Nitrosative and oxidative stresses are perceived by the HcpR2 iron-sulfur cluster resulting in impaired DNA-binding and derepression of *yblA-hcp* expression (Fig. 4b). The *hcp* gene product, Hcp (hybrid-cluster protein), contributes to resisting nitrosative stress.

Accepted

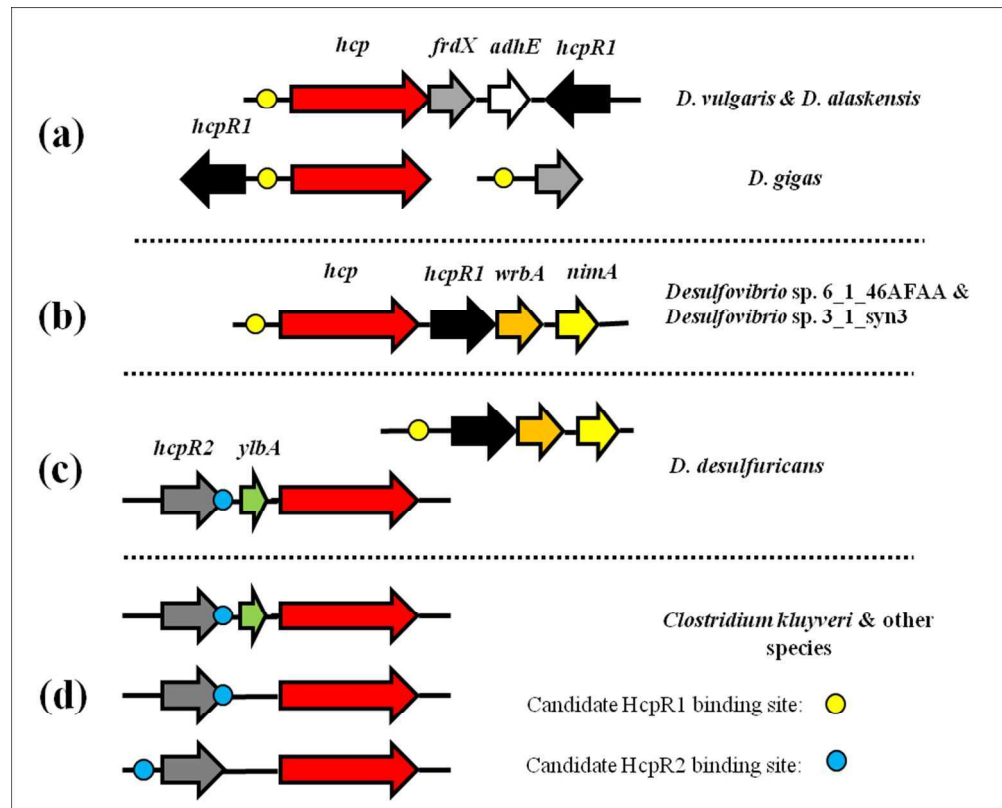


Fig. 1. The genomic loci of *hcpR1* and *hcpR2* in *D. desulfuricans* and closely related species. Arrows represent putative genes. Matching colors indicate conserved genes.

172x138mm (150 x 150 DPI)

Accep

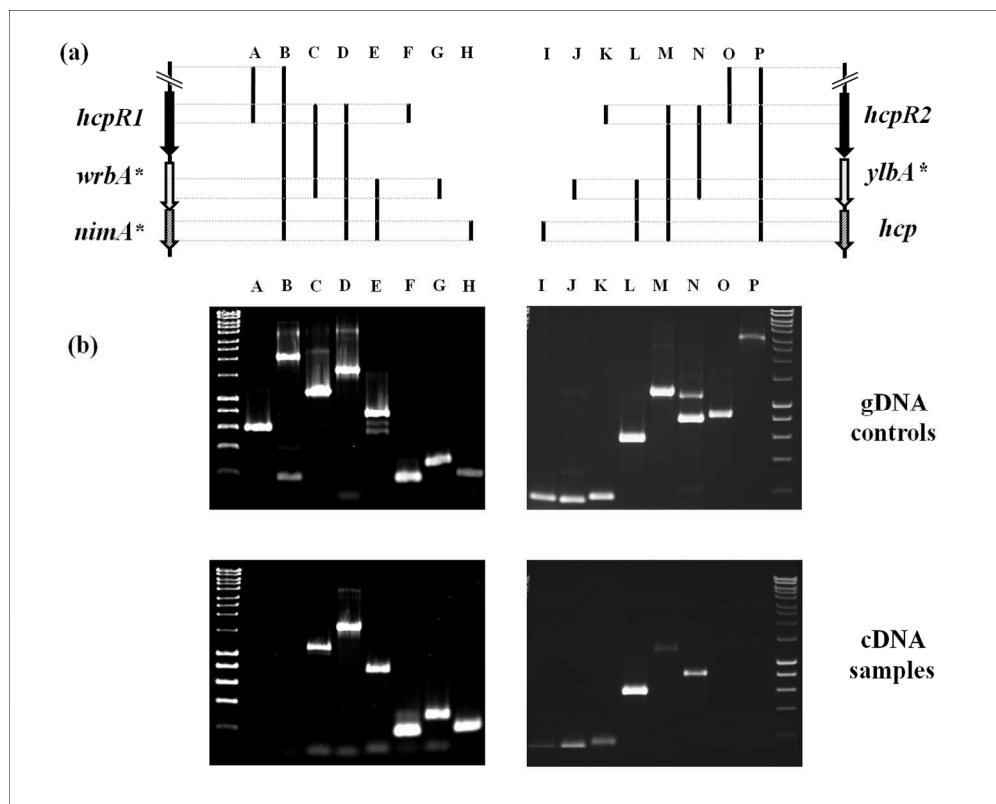


Fig. 2. Transcript mapping of the *hcpR1* and *hcpR2* loci. (a) Primers were designed to amplify DNA fragments spanning the coding regions of the *hcpR1* and *hcpR2* loci. Additional primers, specific to DNA sequences upstream of the putative *hcpR1* and *hcpR2* promoters, were included. Combinations of these primers were expected to generate PCR fragments of different sizes and were allocated a letter A-P. These are represented in the cartoon. (b) Primer combinations were used for a series of PCRs using either *D. desulfuricans* gDNA or cDNA as template. Negative control PCRs using no template DNA were also included. PCR products were resolved by agarose gel electrophoresis. Bioline Hyperladder II was used as a standard on the gel to assess PCR fragment sizes. Fragments of corresponding sizes were generated for all primer combinations when gDNA was used as the PCR template. Fragments were generated for all primer combinations except those utilizing the *hcpR1* or *hcpR2* promoter primers when cDNA from *D. desulfuricans* was used as the template. No fragments were generated when no template was used (data not shown).

252x201mm (150 x 150 DPI)

Acc

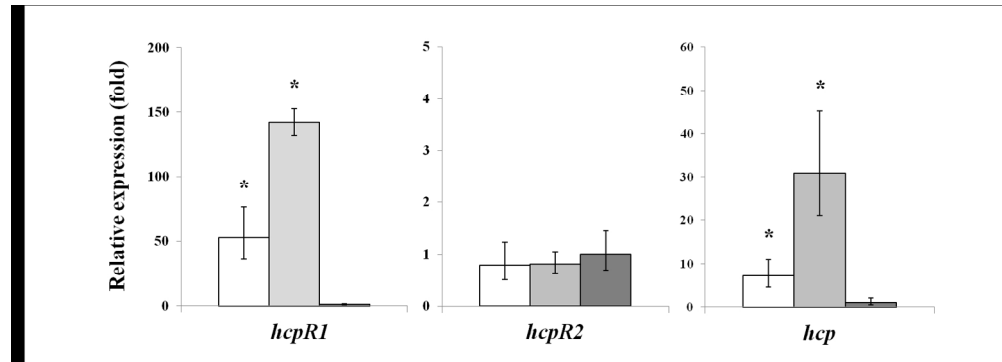


Fig. 3. Effect of the terminal electron acceptor during growth on expression of *hcpR1* and *hcpR2* genes. RNA was purified from samples of early exponential phase cultures of *D. desulfuricans* 27774 grown in media containing 7.5 mM nitrate (unshaded bars) or sulfate (dark grey shading) or 2.5 mM nitrite (pale grey shading) as the only terminal electron acceptor. Transcript levels were determined by qRT-PCR normalized against levels of *polA* mRNA. Expression levels were derived from three biological replicates and triplicate qPCR reactions. Expression levels were normalized to those of the sulfate grown culture. Stars indicate data derived from ΔCt values significantly different to those for sulfate-grown cultures ($p < 0.05$).

296x106mm (150 x 150 DPI)

Accepted

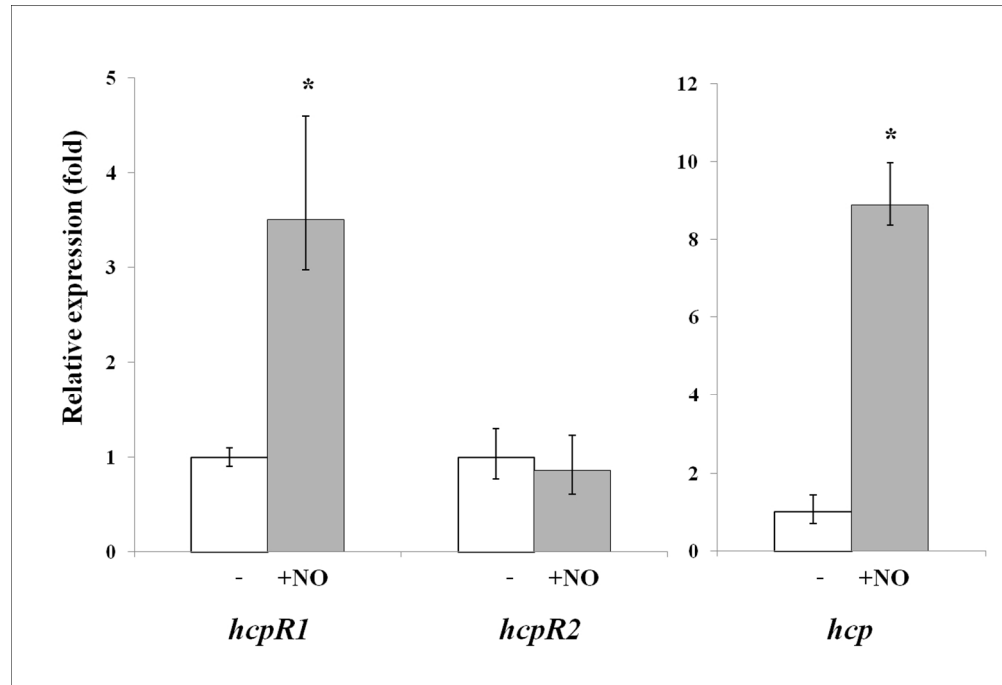


Fig. 4. RT-qPCR of *hcpR* genes in *D. desulfuricans*. Cells were grown on medium containing 15 mM sulfate as the sole terminal electron acceptor. Once cultures reached an OD600 of ~ 0.3 they were treated with 7.5 μM NO. After 20 h the cells were harvested and used for RNA isolation. Total RNA was reverse-transcribed with random hexamers and the resulting cDNA was used for qPCR analysis. Transcript levels were normalized against *poIA* levels and expression levels are derived from three biological replicates and are normalized to those given by untreated sulfate grown cells. (a) levels of *hcpR1* and *hcpR2* mRNA; (b) levels of *hcp* mRNA. Stars indicate data derived from ΔCt values significantly different to that for untreated cultures.

232x158mm (150 x 150 DPI)

Accep

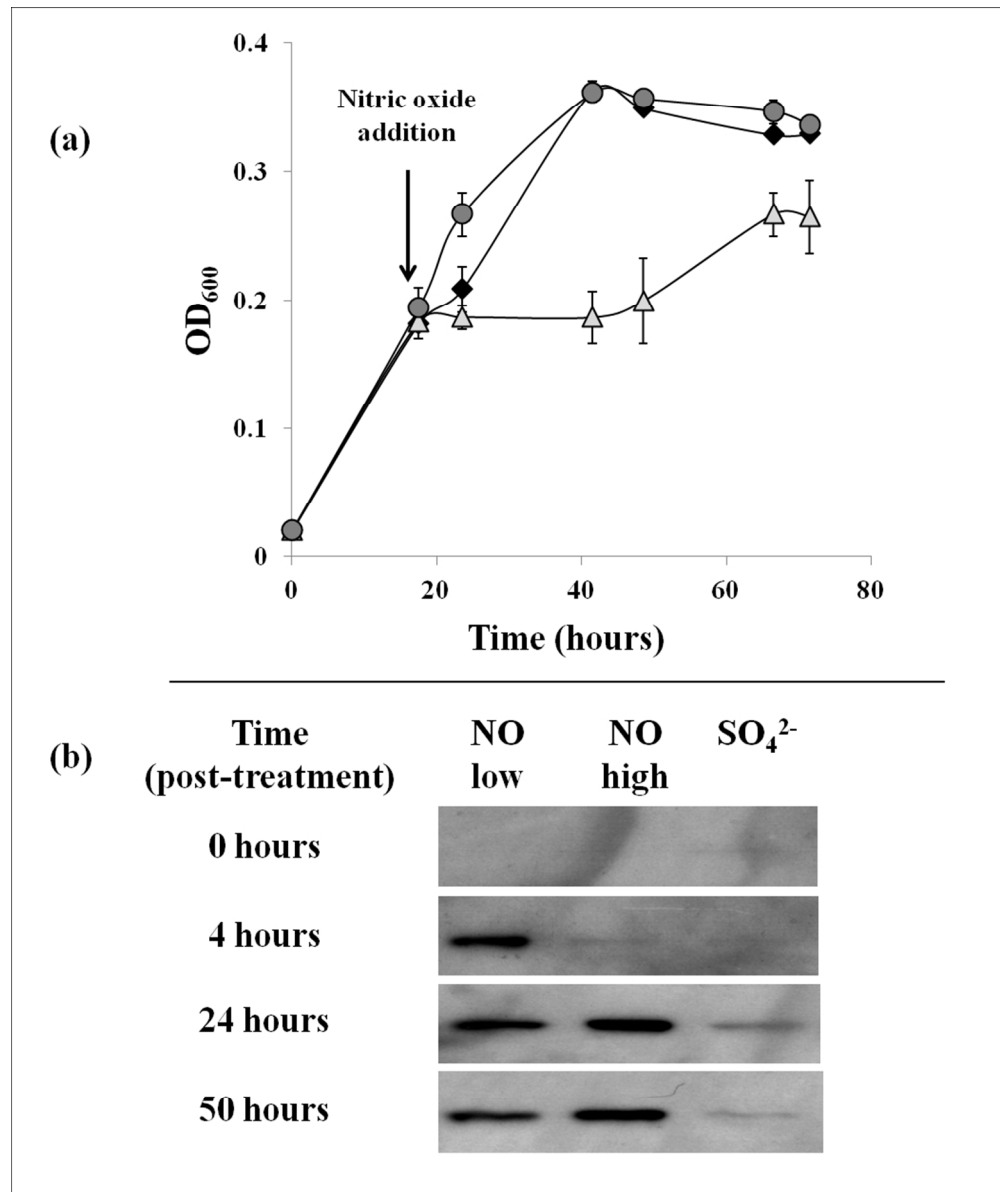


Fig. 5. The effects of exogenous NO on levels of HcpR1 synthesis. (a) Sulfate grown cells were used to inoculate cultures supplemented with 7.5 mM sulfate and cell densities were monitored over time by measuring OD₆₀₀. After 18 h the cultures were treated with a low 5 μ M dose of NO (black diamonds), a high 25 μ M dose of NO (grey triangles) or no treatment (grey circles). Results are the average of three separate biological replicates and error bars indicate standard deviations. (b) Standardized protein samples were prepared from cells harvested at 0, 4, 24 and 50 h post-treatment. Proteins were resolved by SDS-PAGE and used for Western blot analysis using anti-HcpR1 antibodies. Each track was loaded with 3 μ g of soluble cell protein.

178x212mm (150 x 150 DPI)

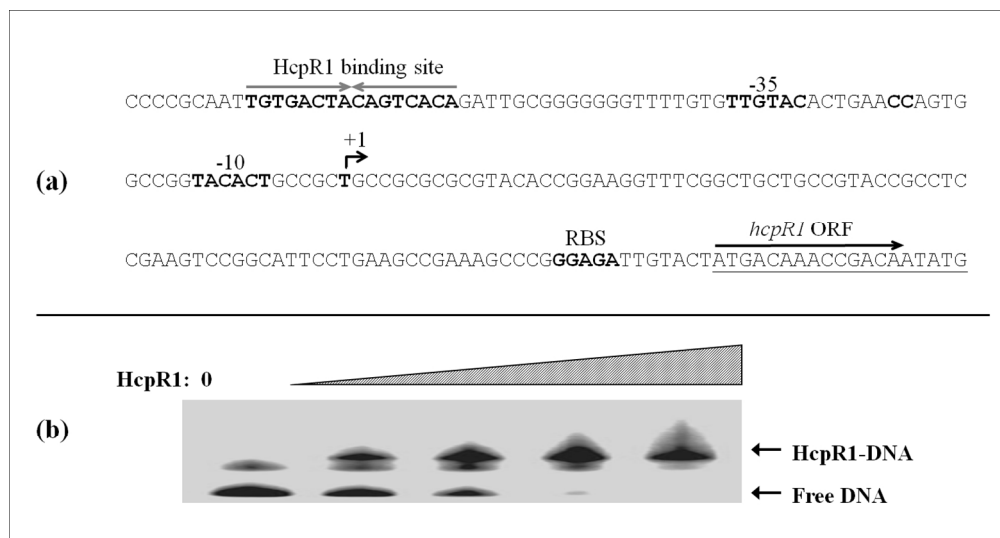


Fig. 6. HcpR1 is a DNA-binding protein. (a) A potential HcpR1 DNA target site was identified upstream of the *hcpR1* gene. Putative -10 and -35 promoter elements and ribosome binding site (RBS) were also identified.

(b) Binding of HcpR1 to a DNA fragment containing the predicted HcpR1 site was assessed by EMSA. ^{32}P -labelled *hcpR1* promoter DNA fragment was incubated with increasing concentrations of HcpR1 and then resolved by non-denaturing electrophoresis. Herring sperm DNA was also included in the incubation mixtures to act as non-specific competitor DNA. HcpR1 was included in the incubations at 0, 25, 50, 100 and 200 nM. Free DNA and HcpR1-DNA complexes are marked with arrows.

254x135mm (150 x 150 DPI)

Accepted

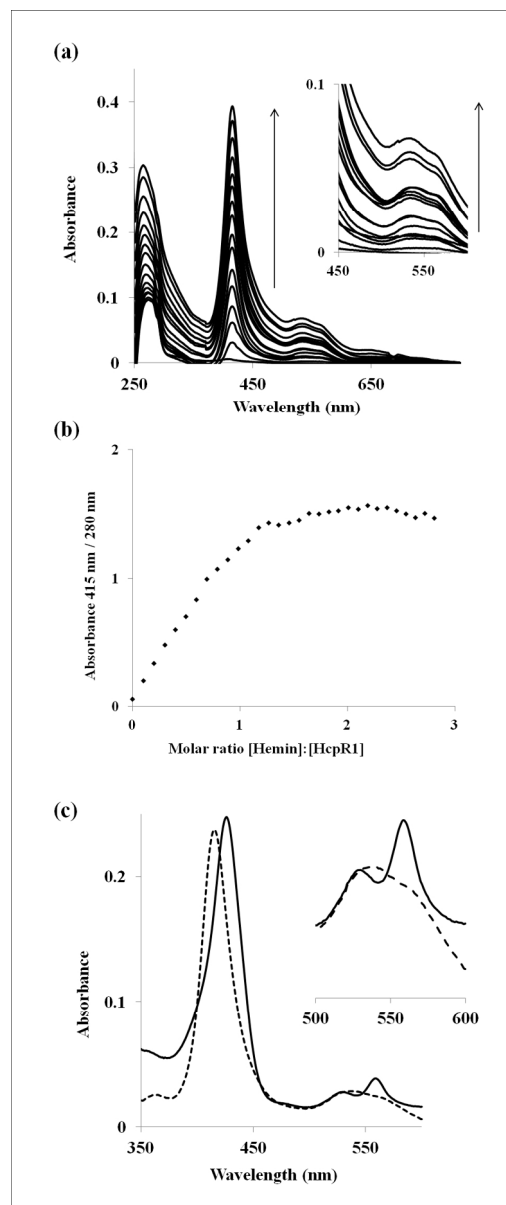


Fig. 7. Binding of hemin to HcpR1. (a) HcpR1 (12.5 μM) was titrated with hemin and UV-visible spectra were recorded against a cuvette containing buffer and a corresponding quantity of hemin. Addition of hemin to HcpR1 resulted in an increase in absorbance at 415 nm, 532 nm and 565 nm, indicating that hemin was bound by HcpR1. Inset highlights the increase in absorbance around 450-600 nm of HcpR1 on addition of hemin. (b) Absorbance at 415 nm, normalized to the absorbance at 280 nm (Chakravarti et al., 2010; Larson et al., 2012), was plotted against the molar ratio of hemin:HcpR1. The plot indicates that HcpR1 was saturated with hemin at a molar ratio of approximately 1.2:1 (hemin:HcpR1) suggesting that HcpR1 binds hemin with a stoichiometry of 1:1. (c) The addition of dithionite to hemin supplemented HcpR1 resulted in a change in the absorbance profile with the peaks shifting to 425 nm, 530 nm and 560 nm. Reduced HcpR1 hemin (solid black line) and non-reduced HcpR1 hemin (broken line).

163x387mm (150 x 150 DPI)

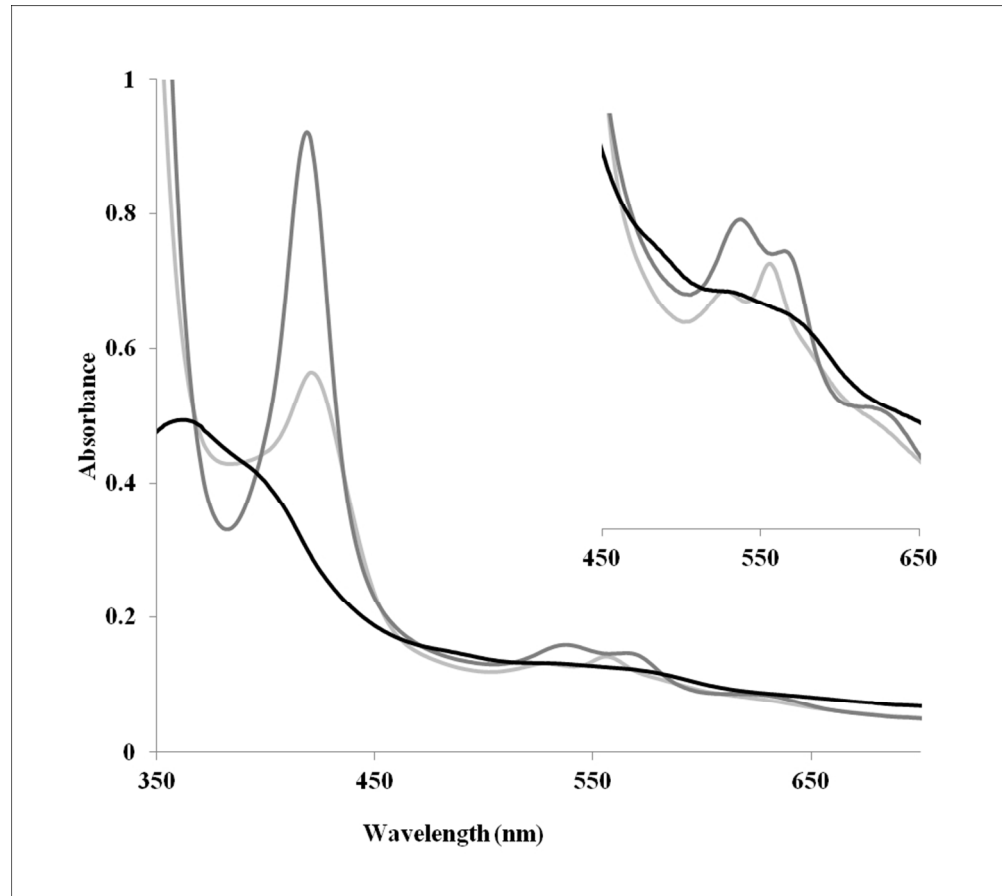


Fig. 8. Binding of NO and CO by the HcpR1 ligated Fe²⁺-heme. HcpR1 (30 μ M) was supplemented with a sub-stoichiometric (10 μ M) quantity of hemin, reduced with dithionite and then a UV-visible spectrum was recorded under anaerobic conditions. Samples were then gently flushed for 1 minute with either CO or NO and additional spectra were recorded. Treatment with CO resulted in a change in the absorbance profile with peaks shifting to 418 nm, 537 nm and 565 nm. Treatment with NO resulted in a loss of absorbance peaks typical for protein-ligated heme suggesting that heme is lost from HcpR1 when bound to NO.

172x154mm (150 x 150 DPI)

Acc

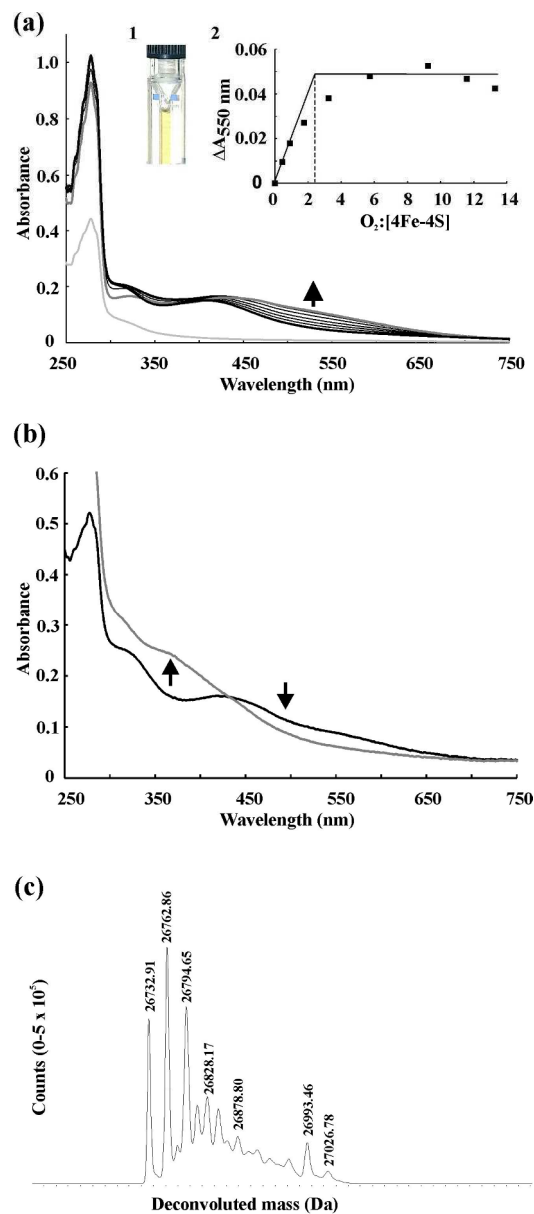


Fig. 9. Reconstituted HcpR2 has spectral properties consistent with the presence of an oxygen- and nitric oxide sensitive iron-sulfur cluster. (a) Apo-HcpR2 was reconstituted as described in Experimental procedures (inset 1). The UV-visible spectrum (heavy black line; $\sim 9.4 \mu\text{M}$ cluster) was typical of a [4Fe-4S] protein. Reconstituted HcpR2 was titrated with aliquots of air-saturated buffer ($220 \mu\text{M}$ O_2 at room temperature) such that the final concentrations of O_2 were 0.0, 4.3, 8.5, 16.3, 30.3, 53.3, 85.85, 107.75, and $123.50 \mu\text{M}$. After each addition the reaction was incubated at room temperature for 10 min before measurement of further spectra (fine black lines). The major change in absorbance associated with conversion of the [4Fe-4S] form (heavy black line) to the [2Fe-2S] form (heavy grey line) is indicated by the \blacktriangleleft arrow. Prolonged air-exposure resulted in the formation of apo-HcpR2 (fine grey line). The changes in absorbance at 550 nm ($\Delta A_{550} \text{ nm}$), representing the appearance of the [2Fe-2S] cluster, are plotted against the ratio of $[\text{O}_2]:[\text{4Fe-4S}]$ in inset 2. The lines join the tangent to the initial slope to the asymptote of the curve; the dashed line indicates the likely stoichiometry of the reaction. (b) Spectra of reconstituted HcpR2 ($\sim 10 \mu\text{M}$ cluster) under anaerobic conditions before (black line) and after 30 min incubation at room

temperature in the presence of 400 μM NO (grey line). (c) Detection of nitrosylated iron-sulfur clusters and nitrosated protein after treatment of reconstituted HcpR2 (initially ~ 10 μM cluster) with NO (~ 400 μM). Samples were analyzed by liquid chromatography-mass spectrometry as described in Experimental procedures. The HcpR2 species corresponding to 14 peaks in the mass spectrum are listed in Table 1.

112x260mm (299 x 299 DPI)

Accepted Article

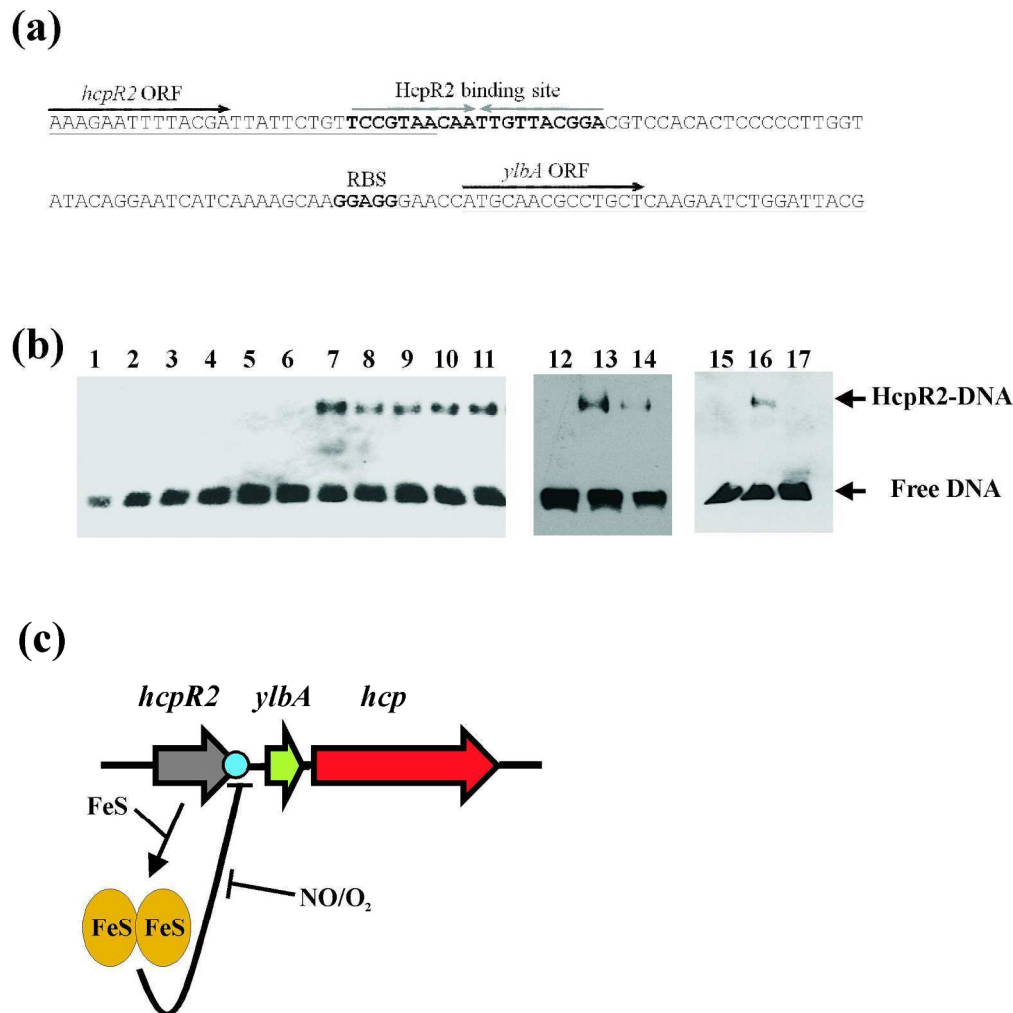
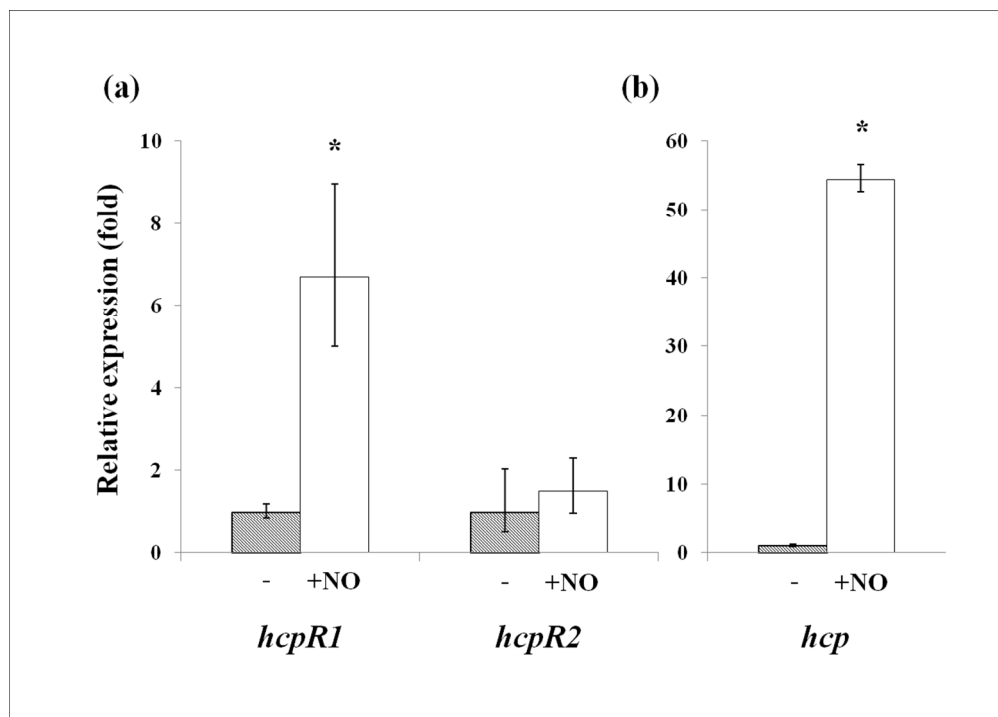


Fig. 10. DNA-binding by reconstituted HcpR2 is impaired by exposure to nitric oxide. (a) A candidate HcpR2 DNA target site was identified in the intergenic region between, and slightly overlapping with, *hcpR2* and the downstream *ylbA*-*hcp* genes. Although a putative RBS binding site was identified, no obvious promoter elements were found. Binding of HcpR2 to a DNA fragment containing this sequence was assessed by EMSA. (b) Effect of the HcpR2 iron-sulfur cluster and NO on DNA-binding. Biotin-labeled promoter DNA fragment was incubated with increasing concentrations of reconstituted HcpR2 and then resolved by non-denaturing electrophoresis under anaerobic conditions. The concentrations of reconstituted HcpR2 (nM dimer; note that HcpR2 eluted as a dimer in size exclusion chromatography experiments) were: lanes 1, 12 and 15, 0; lane 2, 50; lane 3, 100; lane 4, 200 nM; lane 5, 400; lane 6, 500; lane 7, 800; lane 8, 1000; lane 9, 1200; lane 10, 1400; lane 11, 1500; lane 13, 1000 nM HcpR2; lane 14, 1000 nM; lane 15, HcpR2 exposed to NO; lane 16, 1500 HcpR2; lane 17, 1500 apo-HcpR2. Free DNA and HcpR2-DNA complexes are marked with arrows. (c) Model of the regulation of *ylbA*-*hcp* operon by HcpR2 in response to NO- and O₂-mediated stress. The *hcpR2* gene is under low level constitutive transcription. Translation of *hcpR2* mRNA generates apo-HcpR2 which incorporates one [4Fe-4S] cluster per protomer. The [4Fe-4S] form of HcpR2 binds at an inverted repeat DNA sequence (CCGTAACAATTGTTACGGA) located in the *hcpR2*-*ylbA* intergenic region to repress expression of *ylbA*-*hcp*. Nitrosative and oxidative stresses are perceived by the HcpR2 iron-sulfur cluster resulting in impaired DNA-binding and derepression of *ylbA*-*hcp* expression (Fig. 4b). The *hcp* gene product, Hcp (hybrid-cluster protein), contributes to resisting nitrosative stress.

192x194mm (299 x 299 DPI)

Some sulfate reducing bacteria isolated from the human body contain two Crp/Fnr family transcription factors, HcpR1 and HcpR2, that use different sensory mechanisms to regulate their defense against NO-induced nitrosative stress. We propose that acquisition of an additional *hcpR* gene, possibly from another member of the gut microbiome, permits specialization of these regulators to fulfill different roles under selective pressure in the gastro-intestinal tract where they are exposed to multiple sources of nitrosative stress.

Accepted Article



Effect of nitric oxide on the transcription of *Desulfovibrio desulfuricans* genes for the hybrid cluster protein and two transcription factors, HcpR1 and HcpR2, that regulate the response to nitrosative stress.

220x156mm (150 x 150 DPI)

Accept